2008

Relationship Between Arch Height and Midfoot Joint Pressures During Gait

Dong Gil Lee
Cleveland State University

RELATIONSHIP BETWEEN ARCH HEIGHT AND MIDFOOT JOINT PRESSURES DURING GAIT

DONG GIL LEE

Bachelor of Science in Biomedical Engineering

Inje University, South Korea

Master of Science in Medical Radiology

Inje University, South Korea

Submitted in partial fulfillment of requirements for the degree of

DOCTOR OF ENGINEERING IN APPLIED BIOMEDICAL ENGINEERING

at the

CLEVELAND STATE UNIVERSITY

December, 2008

This dissertation has been approved
For the Department of Chemical and Biomedical Engineering
and the College of Graduate Studies by

_____
Dissertation Committee Chairperson, **Brian L. Davis, Ph.D.**
Department of Chemical and Biomedical Engineering

_____
Date

_____
Majid Rashidi, Ph.D., P.E.
Department of Mechanical Engineering

_____
Date

_____
Robert P. Mensforth, Ph.D.
Department of Anthropology

_____
Date

_____
Antonie J. van den Bogert, Ph.D.
Department of Chemical and Biomedical Engineering

_____
Date

_____
Peter R. Cavanagh, Ph.D., D.Sc.
Department of Orthopaedics and Sports Medicine
University of Washington

_____
Date

RELATIONSHIP BETWEEN ARCH HEIGHT AND MIDFOOT JOINT PRESSURES DURING GAIT

DONG GIL LEE

ABSTRACT

A foot arch is a multi-segmented curved structure which acts as a spring during locomotion. It is well known that ligaments are important components contributing to this spring-like property of the arch. In addition, intrinsic and extrinsic foot muscles contribute to arch support. According to the windlass foot model, arch height and midfoot joint orientation change during gait. However, it is not known whether altered joint configurations result in increased joint stress during gait. If so, it is possible for there to be a “vicious cycle” in which joint stress increases as the arch height diminishes, which may then lead to further increases in joint stresses and eventual bone destruction.

The purpose of this study was to examine joint pressure differences of the midfoot in normal and diabetic feet during walking simulation using a robotic system. This study focused on the relative importance of muscles, ligaments and bony structures. Sixteen cadaver foot specimens were used in this study. Joint pressures were measured dynamically during full stance at four medial locations (the first cuneometatarsal, medial cuneonavicular, middle cuneonavicular, and first intercuneiform). Human gait at 25% typical walking speed and 66.7% body weight was simulated with the Universal Musculoskeletal Simulator.

It was shown that diabetic cadaver feet had, on average, a 46% higher peak in pressures, than control cadaver feet across all four tested joints. There were inverse correlations between the arch height and the peak joint pressure during the simulated arch collapse. It was proven that the acquired flat foot, caused by the tibialis posterior dysfunction, caused medial peak joint pressure increase by 12% across all tested joints.

These results could be used in furthering our understanding of the etiology of diabetic foot diseases. Also, these findings could suggest better treatment for diabetic patients, who are at risk for Charcot foot abnormalities.

TABLE OF CONTENTS

LIST OF TABLES

LIST OF FIGURES

CHAPTER I

INTRODUCTION

1.1 Significance

As the diabetic population gets larger, diabetic foot problems are becoming increasingly severe (Davis *et al.*, 2004). Despite extensive efforts on the part of physicians and scientists to understand such devastating complications, Charcot Neuroarthropathy (CN) is one complication where the exact etiology is still unidentified. Thus far, all we know is that CN is a destructive process mainly associated with neuropathy of the feet and ankles in diabetic patients. This progressive joint disease results in permanent foot deformity (Caputo *et al.*, 1998). Over 70% of CN cases have been found at the first ray and midfoot area; areas which are most vulnerable to distorted architecture and foot arch collapse with progression of the disease (Trepman *et al.*, 2005; Rajbhandari *et al.*, 2002). Furthermore, patients who have neuropathy of the foot have a decreased sense of pain in the foot. As a result, a patient will continue to walk with the deformed foot, possibly adding to the structural collapse. With a deformed foot and the absence of pain, patients' daily activity without treatment accelerates development of

complications such as midfoot ulceration. As the deformation process proceeds, the curved beam shape of the midfoot structure will experience a pressure change during standing and running. However, it is not yet verified how much pressure the joints experience during process that results in a CN deformity.

In order to understand underlying risk factors, it is necessary to verify mechanical changes *in vivo*. Most of these studies have focused on parameters measured from outside of the foot due to ethical issues. For this reason, most researchers prefer to conduct computational simulations to estimate *in vivo* mechanical parameters; yet, these computational simulations have inherent limitations such as lack of control and assumption for an internal organ's function and geometry. Therefore, this cadaver study could provide unique opportunities to understand internal foot mechanics during simulated walking.

1.2 Objective

The purpose of this study was to examine pressure difference at joints of the midfoot in normal and diabetic feet during simulated gait using a robotic system. This study focused on the relative importance of muscles, ligaments and bony structure in determining arch height and joint stresses.

1.3 Specific aims

Aim 1: Build a musculoskeletal robotic system, which simulates stance phase of gait with cadaveric feet.

Aim 1 focused on the engineering aspect in order to build a musculoskeletal

robotic system, which consists of the 6-degrees-of-freedom parallel robotic system and multi tendon actuators. These hardware components required critical timing and synchronization of the interface between hardware components and control software. This challenge was accomplished using programming in LabVIEW.

Aim 1 included the following study:

- Integrate the parallel robotic system with multi tendon actuators.
- Build a control software using LabVIEW development environment.

Aim 2: Investigate the relationship between arch height and joint pressures of the midfoot during gait among various cadaveric feet.

Ligaments and tendons in the foot act as a tension band and an inverter to support the arch of the foot. We dissected and disengaged major foot ligaments and tendons to simulate arch collapse and observed concomitant joint pressure changes of the midfoot during gait. In addition, we compared joint pressures of the midfoot in normal and diabetic feet in order to elucidate the effect of diabetes on midfoot joint pressures.

Aim 2 studied the following:

- Compared joint pressures of the midfoot in normal and diabetic feet.
- Measured joint pressures of the midfoot at different foot conditions.

The research hypotheses in this study are:

Hypothesis 1. Joint pressures of the midfoot are higher for diabetic subjects than the normal population due to increased stiffness of soft tissues and limited range of joint motion.

Hypothesis 2. The induced arch collapsing results in higher joint pressures of the midfoot during walking simulation.

1.4 Dissertation outline

The outline of the dissertation can be summarized as;

I. New Control Software for a Robotic Gait Simulator (Chapter 2)

II. Assessment of Effects of Diabetes on Joint Pressures of the Midfoot Using a Robotic Gait Simulator (Chapter 3)

III. Determination of Joint Pressures of the Midfoot Using a Robotic Gait Simulator: Diabetic Differences and Artificially Induced Flatfoot Deformities (Chapter 4)

IV. The Impact of Tibialis Posterior Dysfunction on Joint Pressure of the Midfoot (Chapter 5)

1.5 References

Davis, B.L., Kuznicki, J., Praveen, S.S., Sferra, J.J., 2004. Lower-extremity amputations in patients with diabetes: pre- and post-surgical decisions related to successful rehabilitation. Diabetes Metabolism Research and Reviews 20 (Suppl 1), S45-S50.

Caputo, G.M., Ulbrecht, J., Cavanagh, P.R., 1998. The charcot foot in diabetes: six key points. American Family Physician 57 (11), 2705-2710.

Trepman, E., Nihal, A., Pinzur, M.S., 2005. Charcot neuroarthropathy of the foot and

ankle. Foot & Ankle International 26 (1), 46-63.

Rajbhandari, S.M., Jenkins, R.C., Davies, C., Tesfaye, S., 2002. Charcot neuroarthropathy in diabetes mellitus. Diabetologia 45 (8), 1085-1096.

CHAPTER II

NEW CONTROL SOFTWARE FOR A ROBOTIC GAIT SIMULATOR

Dong Gil Lee, Robb W. Colbrunn, Antonie J. van den Bogert, and Brian L. Davis

Computer Methods & Programs in Biomedicine, to be submitted.

2.1 Preface

New LabVIEW based control software was developed to control a robotic gait simulator which can recreate walking motion with cadaver specimens. The control software included various functions to control a parallel robot and multi- tendon actuators to apply physiological loads on cadaver specimens in order to recreate realistic walking. In addition, this software allowed researchers to investigate various *in vitro* factors during simulation with cadaver specimens. This control software integrated and synchronized many hardware devices into a single program using multiple independent functions. A number of cadaver studies have been successfully performed by the control software. These results could contribute to an enhancement of our understandings and suggestions for many foot and ankle related clinical questions. Furthermore, this robotic system could be used to verify surgical trials for orthopaedic research.

2.2 Abstract

New LabVIEW based control software was developed to control a robotic system that can recreate human walking motion using a cadaver specimen. The software was able to both (i) control a parallel robot to recreate physiologically-correct kinematic trajectories and (ii), control multi- tendon actuators to apply physiological loads to tendons traversing the ankle joint in order to recreate realistic walking. This control software was designed to provide various opportunities for researchers to investigate mechanical and physiological factors during simulated walking using a cadaver specimen. Results from studies that utilize this system to investigate midfoot joint contact pressures, ligament stretch and/or other biomechanical variables could greatly enhance our understanding of foot disorders ranging from flat foot deformities to Charcot joint disease or metatarsal stress fractures. Furthermore, this system could be used to perform surgical trials for orthopaedic research.

2.3 Introduction

Many different types of robotic systems have been developed to simulate human gait using cadaver specimens for over a decade (Nester *et al.*, 2007; Hurschler *et al.*, 2003; Kim *et al.*, 2001; Sharkey *et al.*, 1998). These robotic cadaver gait simulators could provide unique opportunities to investigate orthopedic research questions, including (i) the ability to provide realistic data for verifying mathematical and computational models, (ii) testing the effectiveness of new surgical techniques by examining various mechanical consequences after performing surgery on cadaver specimens, and (iii) studying injuries such as joint sprains, avulsion fractures and fatigue-

induced stress fractures. Since these studies are performed with cadaveric specimens these studies circumvent ethical issues related to causing injury in healthy subjects.

While a few research articles focus on the progress of hardware components and control algorithms which make it possible to recreate more realistic human motions using cadaver specimens (Aubin *et al.*, 2008), there are few publications pertaining to the presentation of the control software for these robotic systems. It can be speculated that most researchers develop and use software, piece by piece, for different hardware components or different process steps. Creating custom adaptations of this fragmented software depending on the scientific question could minimize developing time, but the fragmented software will likely require additional work, during the actual experiment, to transfer data system-to-system and to process data at different steps. This fragmented approach limits the ability to recreate certain activities of daily living compared with a more general foot and ankle simulator. Moreover, fragmented software could develop synchronization problems while operating different hardware components simultaneously in real time. The purpose of this research paper is to introduce new integrated control software, which has the functionality of controlling all motion-generating hardware components as well as external data acquisition systems synchronously to provide a flexible and accurate simulation test bed for cadaveric foot and ankle simulations. This particular control software has been originally developed as a subset of the Universal Musculoskeletal Simulator (UMS) for a number of human joint simulation studies. Though this manuscript focuses on gait simulations, it is important to note that as a subset to the UMS the control software encompasses a system which is able to simulate jumping, landing, and other motions of interest to foot and ankle researchers.

2.4 Research materials and methods

System operation description

The major hardware of the UMS consists of a six-degree-of-freedom parallel robot (R-2000, Parallel Robotic System Corporation, Hampton, New Hampshire), a force plate (4060A, Bertec, Columbus, Ohio), a microscribe (G2L, Immersion Corporation, San Jose, California), a rotary type Achilles tendon actuator (BSM80N-275AE servomotor, Baldor, Forth Smith, Arizona / CSG-40-50 harmonic drive, Harmonic Drive Systems, Hauppauge, New York), and four linear type tendon actuators (SM233A servomotors and ET-50 series actuators, Parker, Rohnert Park, California) (Fig. 1). In order to recreate a walking motion, the tibia was fixed horizontally on the UMS frame and the force plate was mounted vertically on the top of the parallel robot's platform to create an inverted ground-tibia motion. This approach provided two major benefits; (i) it did not require rotating the entire tendon actuator system in accordance with the tibia motion during walking simulation, and (ii) due the parallel robot's unique ability to provide large rotations in the horizontal plane the inverted walking motion was able to adequately simulate full stance.

Figure 2.1. The UMS with a horizontally mounted cadaver foot specimen.

The microscribe provided 3-D information (x, y, z) about the center of the robot's platform, the location and posture of the vertically mounted force plate, and the location and size of the mounted specimen. Based on these measured coordinates, the control software created 4×4 transformation matrixes for the defined coordinate systems of the UMS. These coordinate systems were then used to generate the parallel robot's trajectory using normalized desired kinematic trajectories acquired from a gait lab setting. Five tendon actuators provided muscle forces during simulated walking. The following muscle forces were generated by the tendon actuators (the triceps surae, tibialis posterior, tibialis anterior, flexor hallucis longus, and peroneus longus). Initial muscle force patterns were generated manually based on published reference graphs and scaled to create normalized kinetic trajectories (Perry, 1992). The desired kinetic and kinematic trajectories were normalized to physiological parameters such as foot length, foot width, and body weight. The control software acquired all force data at 1000 Hz sampling rate

by a PCI-6034E DAQ board (National Instruments, Austin, Texas). The resulting Ground Reaction Force (GRF) data from a simulation were collected from the vertically mounted force plate and compared to the desired GRF profiles that were collected in the gait lab. The optimization algorithms were then used to adjust the kinetic and kinematic trajectories to provide GRF convergence.

Control software description

The control software for the foot test bed was developed by programming in LabVIEW (National Instruments, Austin, Texas). The control software involves the manipulation of the parallel robot, five tendon actuators, data acquisition, data signal processing, data display, and communication to other measurement computers. In addition, the control software is built upon a common UMS platform of independent-functional sub-VI's that can be directly used for other orthopedic studies, such as the knee, shoulder, hip, and spine experiments. The main screen consists of five sub tabs: configure tendon actuator tab (Figure 2.2), experiment setup tab (Figure 2.3), run experiment tab (Figure 2.4), optimization tab (Figure 2.5), and advanced device control tab (Figure 2.6).

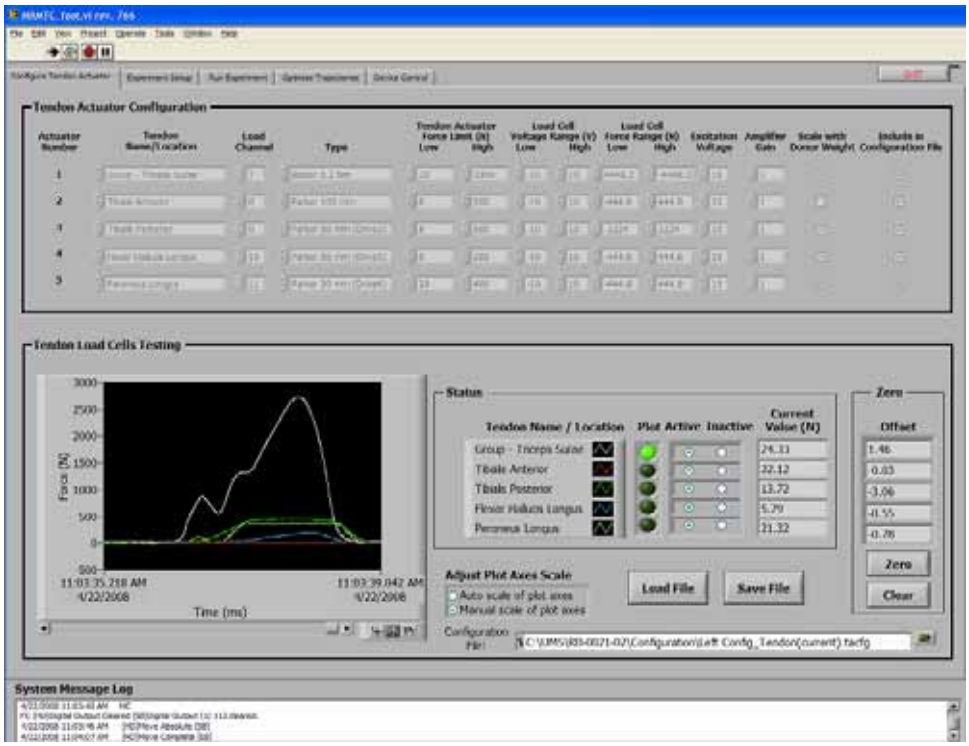

Figure 2.2. Screen view of the configure tendon actuator tab.

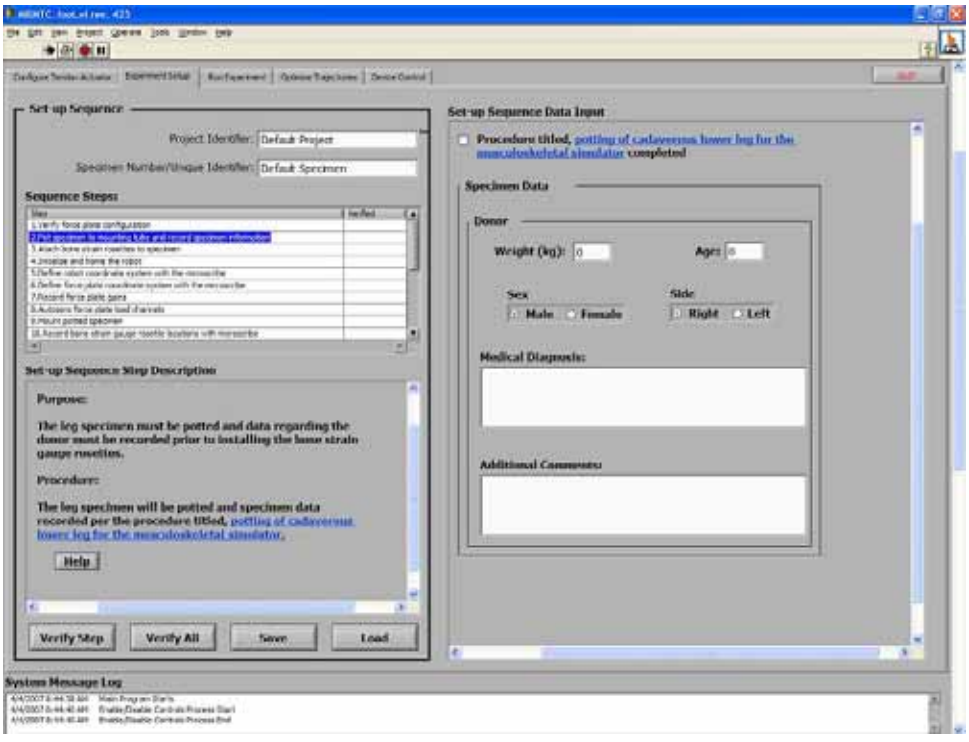

Figure 2.3. Screen view of the experiment setup tab.

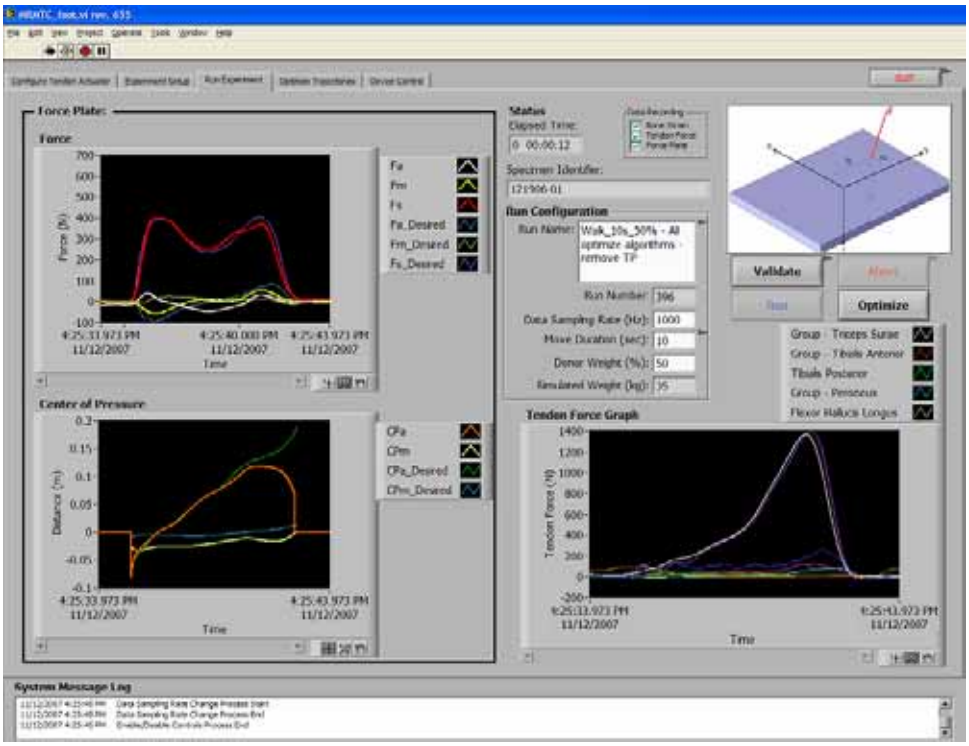

Figure 2.4. Screen view of the run experiment tab.

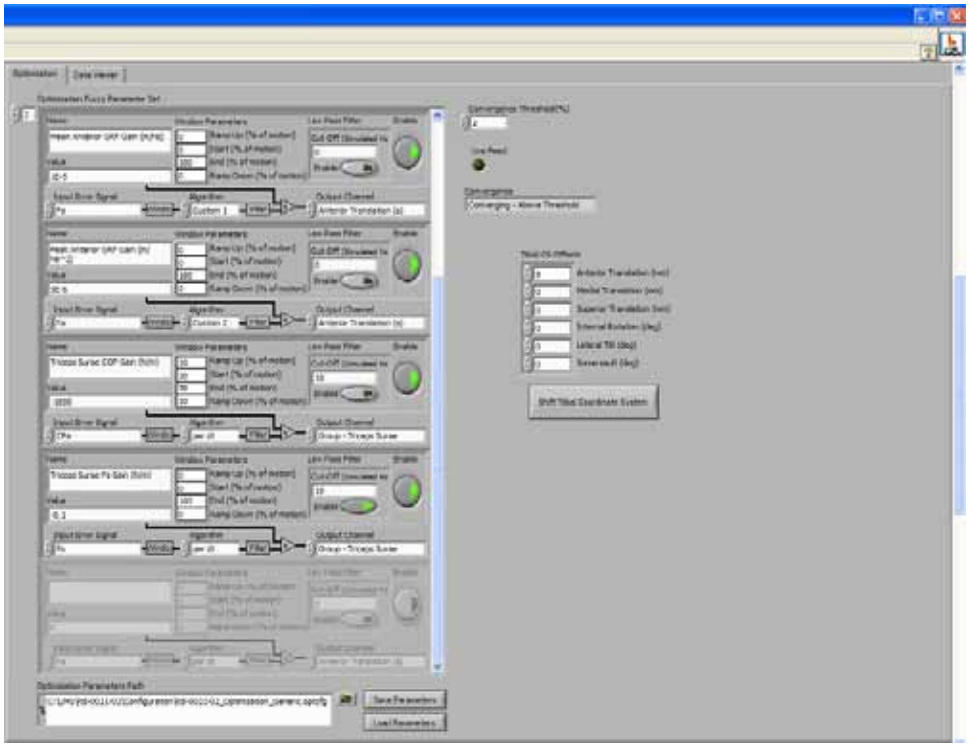

Figure 2.5. Screen view of the optimization tab.

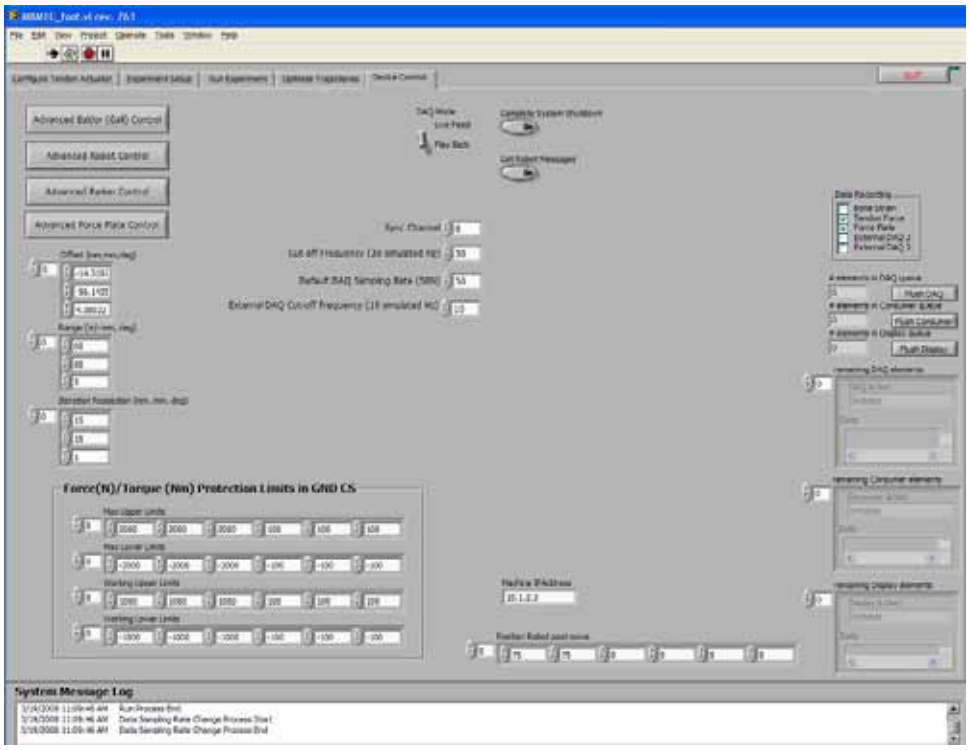

Figure 2.6. Screen views of the advanced device control tab.

The “configure tendon actuator tab” was designed to setup and calibrate multiple tendon actuators. This tab shows current tendon setup status and displays the output signal from each load cell in order to calibrate gains in the amplifier circuit for each tendon actuator in real time. All configuration information was stored in a platform independent ‘.ini’ file format. In order to access all information conveniently, a tendon actuator functional global variable (LabVIEW programming construct) was developed. This allows users to programmatically set and get any tendon actuator’s configuration at any time and any place during the experiment. Additionally, the tendon actuator functional global variable is capable of computing calibration equations for each load cell automatically in real time. For example, if users want to test a specimen employing the same previous conditions, they simply need to load the previous tendon actuator

configuration file. In this way, users can test various specimens using the same experimental protocol without repeating the same tendon actuator setup process. Another functional feature is a force windowing ability of the tendon profiles. This allows users to set a maximum and a minimum tendon force for each tendon actuator in order to prevent overloading and the resulting rupture of tendons. The windowing functionality gives users the capability to easily simulate some pathological tendon activity, such as the tibialis posterior insufficiency, by adjusting the maximum tendon force.

An "experimental setup" tab was designed to manage the setup sequence during the experiment. In order to test various specimens at similar experimental conditions, it was required to define a standard procedure. The standard setup steps were chosen to allow users to define experimental conditions conveniently and consistently. Full descriptions and pictures were implemented to show users how to setup each parameter without requiring additional documentation. In addition, some steps provided hyperlinking capabilities to supporting documentation and picture files, such as *.doc, *.pdf, *.bmp, and *.jpg, to provide more comprehensive information. The following 21 setup steps for the foot experiment were defined:

1. Verify force plate configuration
2. Prepare specimen in mounting tube and record specimen information
3. Attach sensors to specimen
4. Initialize the robot
5. Define robot coordinate system using the Microscribe
6. Define force plate coordinate system using the Microscribe
7. Record force plate gain

8. Autozero force plate load channels

9. Mount potted specimen

10. Record sensor locations using Microscribe

11. Record tibia/fibula landmark using Microscribe

12. Balance sensor signals

13. Load tendon actuator configuration

14. Zero tendon load cells

15. Zero sensor signals

16. Move force plate to the neutral position

17. Record the robot neutral position

18. Record foot neutral position using Microscribe

19. Attach actuators to tendons

20. Enter exercise profile, desired force plate profile, and tendon profile

21. Enter optimization parameters

Some of the steps of the setup sequence can be completed in any given order; however, others need to be completed in a specific order to prevent an inaccurate setup. For example, step 11 must occur after step 9, but nothing is a prerequisite for step 21. This experimental setup step contains a heuristic function where it checks for the completion of prerequisite steps prior to running the requested steps. In the case where an invalid request was made, the function flags the calling function to skip the requested action and return a message to the user listing the prerequisite steps. If re-entering data for a prerequisite step invalidates the data already collected, then the data from those subsequent steps are considered invalidated until the proper sequence is re-executed. This

logic was built based on a Parent-Child tree structure (Figure 2.7). All “Parents” must be verified before any “Child” processes are allowed to execute. Likewise, any changes to any Parent processes invalidate any completed verifications on the Child process. This method created nested situations where one process being re-executed may cause multiple steps to become invalid. This function captured and executed checks at all grandchild and great-grandchild level configurations, not just the child of the modified parent. All configuration data collected during the setup process was stored in memory using the setup functional global variable and also was saved in the ‘.ini’ format.

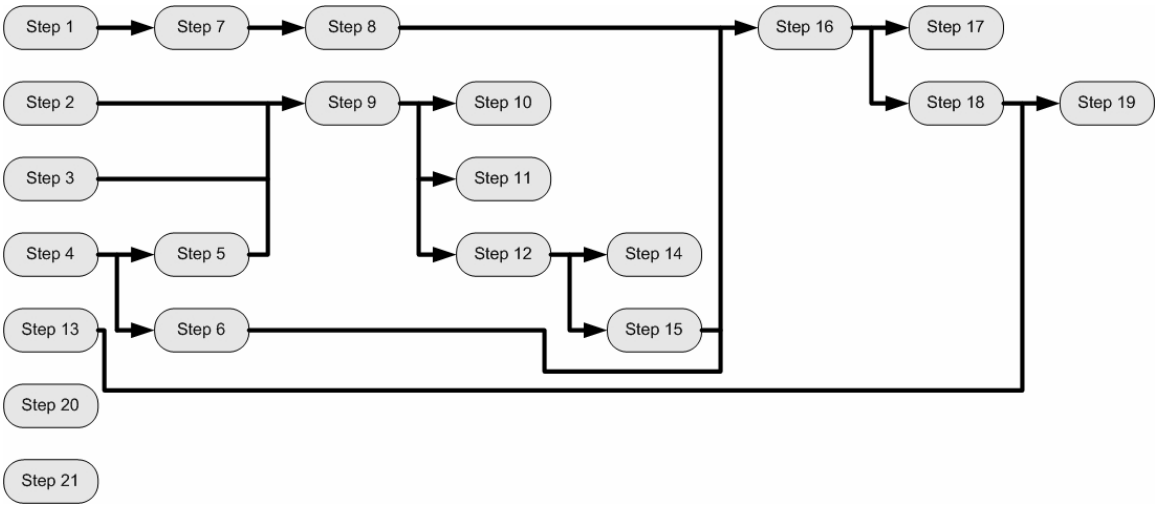

Figure 2.7. The Parent-Child tree structure for the experimental setup step.

The “run experiment” tab is the option used most frequently. The tab was designed to setup DAQ parameters and to retrieve kinetic data during the experiment. In this tab, users can easily modify duration of the stance as well as scale body weight in order to recreate different walking conditions. It displays adjustable error range windows, which lets users verify whether the results of the simulation converged to within the

allowed error ranges. Geometrically, right and left feet have a mirror reflection image of each other. In order to simulate right and left feet, a mirror function was implemented on the setup steps and data viewers. This allows for easy use and comparison of input and resulting data. Coordinate systems were defined in anatomical terms and as a result were mirror-reflected for different anatomical sides in the UMS reference frame. This results in a left handed coordinate system for the left foot and right handed for the right foot. Due to the mathematical need for a right handed coordinate system the mirror function reflected the left handed coordinate system into a right handed coordinate system to provide the correct robot motion and data interpretation for a consistent right foot based data view. The control software also included a path pre-planner that determined the optimum place for the foot to plant on the force plate such that the path was within the robot range of motion. The pre-planner also had the ability to determine which path provided the minimum accelerations for the robot motors in order to create the fastest simulation possible. The "run experiment" tab had a number of controls to select specific desired and actual kinetic data while using the same chart for comparison. Since this tab is the main screen during the experiment, a file manager functional global variable was implemented to automatically save kinetic data after every single run based on the number of executions and additional run parameters. In addition, it automatically saved, processed, and displayed the kinetic and kinematic data after each walking simulation. The kinetic data were conditioned by a zero-phase low pass filter. GRF data were additionally processed to remove gravitational cross-talk on the force plate as the orientation changed throughout the trajectory. This automatic post processing function allows users to save and verify data during experimentation without an additional user's

intervention. It also makes possible the use of this data for optimization of the trajectories.

The “optimization” tab was designed to calculate optimized robot and tendon actuator trajectories based on data from a previous run and the desired trajectory. The basic concept of this optimization process was a trial and error procedure: the procedure was designed to permit repeated “run and adjustment” trials until the results converged. The optimization algorithm is a combination of individual configurable fuzzy logic type controllers (Figure 2.8). Each controller uses one input and one output. A number of configurable fuzzy logic type controllers were implemented to allow users to compensate for errors using a combination of optimization parameters. In addition, each controller had various mathematical signal processing functions, such as adjustable windowing, algorithm (error per dt, mean of error, or custom functions) zero-phase low pass filter, and gain parameter to produce the optimized output trajectory. The output signal was then added to the chosen simulator channel. A number of inputs and outputs can be selected when building these controllers (Table 2.1).

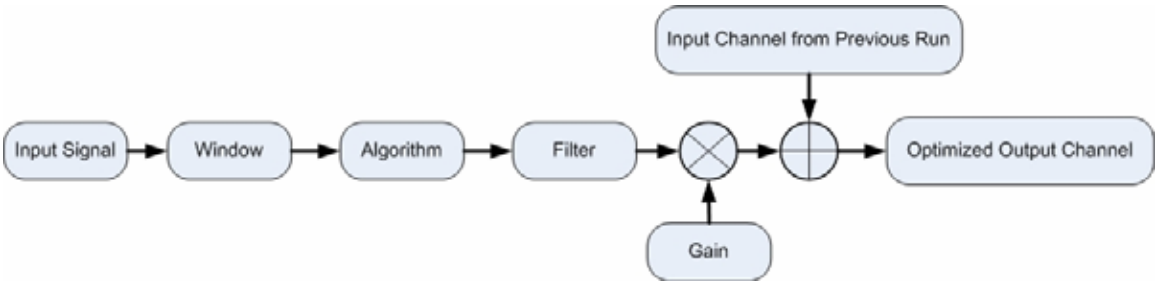

Figure 2.8. The flow chart of the optimization process.

Table 2.1. Input and output parameters for the optimization process.

Controller Input Signals	Controller Output Channel
Anterior GRF (Fa) Error	None
Medial GRF (Fm) Error	Anterior Translation (a)
Superior GRF (Fs) Error	Medial Translation (m)
Anterior COP (CPa) Error	Superior Translation (s)
Medial COP (CPm) Error	Internal Rotation (r)
Internal Rotation Moment (Tr) Error	Lateral Tilt (t)
Constant (1)	Somersault (o)
Linear Ramp (0 to 1)	Group Triceps Surae Force
Linear Ramp (-1 to 1)	Group Tibialis Anterior Force
Linear Ramp (-1 to 0)	Group Flexor Longus Force
	Group Peroneus Force
	Group Extensor Longus Force
	Gastrocnemius Force
	Soleus Force
	Tibialis Anterior Force
	Extensor Digitorum Longus Force
	Extensor Hallucis Longus Force
	Peroneus Tertius Force
	Tibialis Posterior Force
	Flexor Digitorum Longus Force
	Flexor Hallucis Longus Force
	Peroneus Longus Force
	Peroneus Brevis Force

The “advanced device control” tab was designed to provide independent control over each unit of hardware. If any device generates a critical error during the experiment, users would need to investigate the anomaly using low level control over the suspect device. This tab has multiple communication terminals that are connected to each device for error debugging. In addition, this tab has additional setup controls for hardware re-

initialization and specific parameter control. For example, three low level control programs are implemented in this tab in order to manipulate the parallel robot and two different types of the tendon actuators. These programs used the dynamic link library, TCP/IP and ActiveX communication methods to interface the devices. These programs were designed to be used as independent software for the future applications. In addition, this tab had a function to establish a communication for many external data acquisition sub-computers. This feature gives users the ability to measure many different types of physiological parameters simultaneously during the simulation. In order to synchronize the entire system, the low level programs of the parallel robot, tendon actuators and sub-computers were coded to start process at the moment when the parallel robot's controller generates an electric falling trigger signal.

To achieve fast execution and provide multi-thread capability, the control software was divided into four functional sub routines (Multiple queued state machine – producer consumer architecture): user event loop (Producer loop), DAQ loop (1st Consumer loop), processing loop (2nd Consumer loop), and display loop (3rd Consumer loop) (Figure 2.9). Each functional sub routine works independently and in parallel with the others. This programming architecture is designed to take advantage of multi-core processor computing capabilities. For example, the "user event loop" detects user input at the windows level and then sends one or more commands to different target subroutines, thus allowing each core to operate in parallel on the code in each consumer loop. The DAQ loop defines the sampling rate for data acquisition, gets data from the A/D board, and saves data files on the main computer. The "processing loop" executes sub-VIs for data processing and communicates with external controllers and data acquisition

computers. The “display loop” only accepts display commands in order to show data or reconfigure the screen. This separated, parallel structure allows the main computer to execute two or three different tasks simultaneously. As a result, performance of the program is improved by minimizing execution time and maximizing CPU performance.

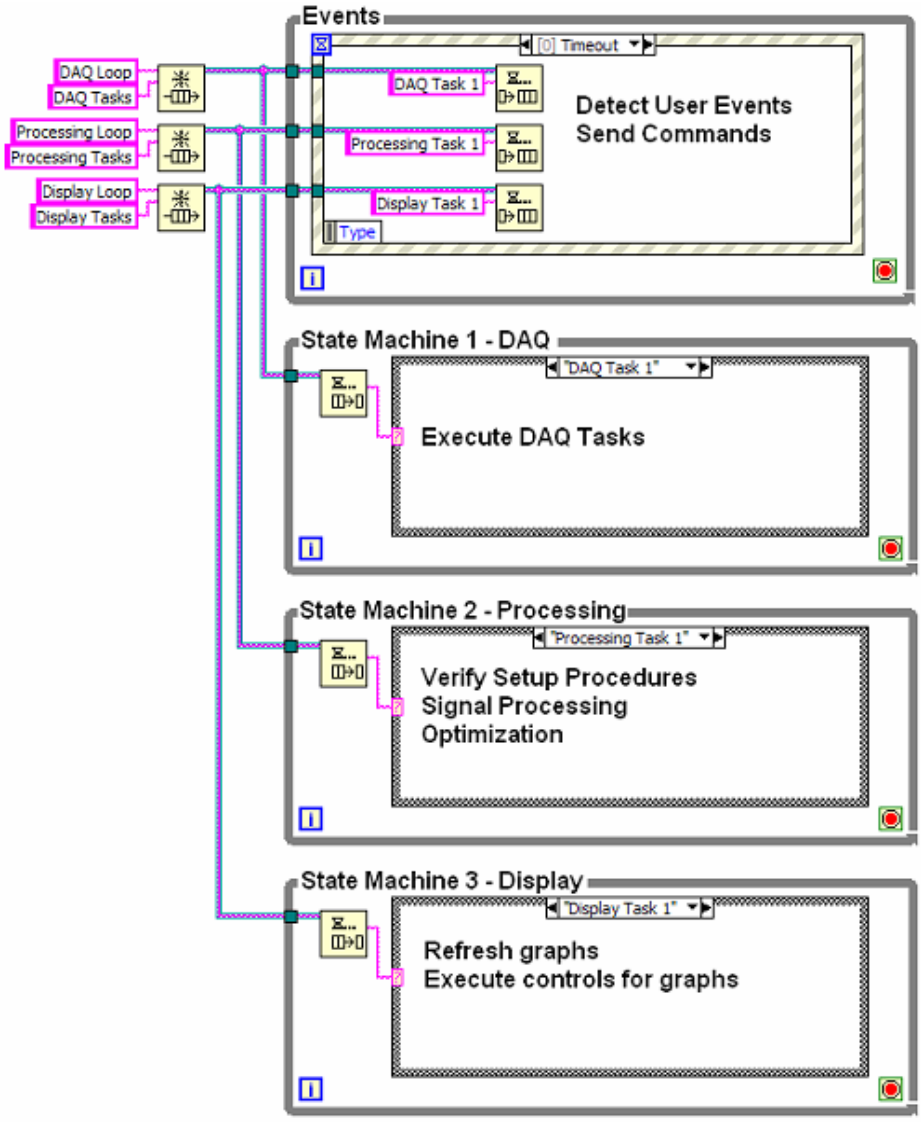

Figure 2.9. Pseudocode of the control software. This programming architecture was based on the multiple queued state machine – producer consumer architecture.

2.5 Results

The common requirement of these cadaver projects was to recreate a realistic walking motion with the UMS and cadaver foot specimens. The full stance phase of walking with realistic physiological conditions was simulated. The UMS walking profile was provided by measuring GRF and kinematic motion from a living subject's walking. The magnitude of the tendon profiles were generated based on the simulated body weight. In most walking simulations, the GRF data was able to be optimized to within +/-10% in the vertical axis and provide similar behavior in the other axes. Created superior ground reaction force and muscle force data are shown in Figure 2.10.

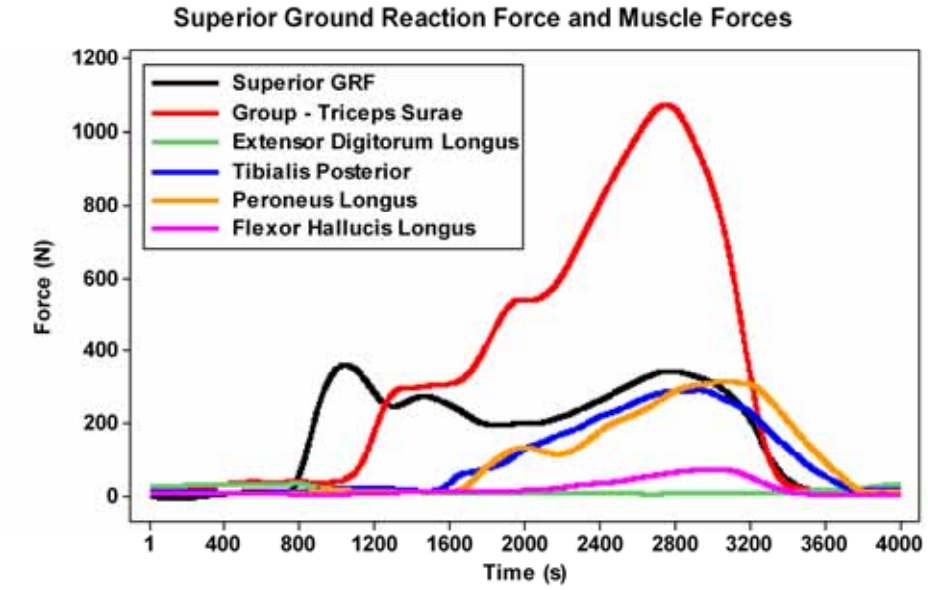

Figure 2.10. Superior ground reaction force and five extrinsic muscle forces during walking simulation.

Joint pressure measurement during walking simulation

Flatfoot and high-arch feet have been recognized as problematic foot conditions that result in foot pain during daily activities. However, it is not completely understood how the mechanical pressure changes in the foot joints during walking in various foot conditions. In order to provide a scientific answer about this clinical question, four medial joint pressures were measured dynamically during walking simulation. The control software was used to simulate walking with a number of cadaver specimens and to communicate with the external joint pressure measurement software. The joint pressure patterns at the midfoot during walking simulation were presented in Figure 2.11.

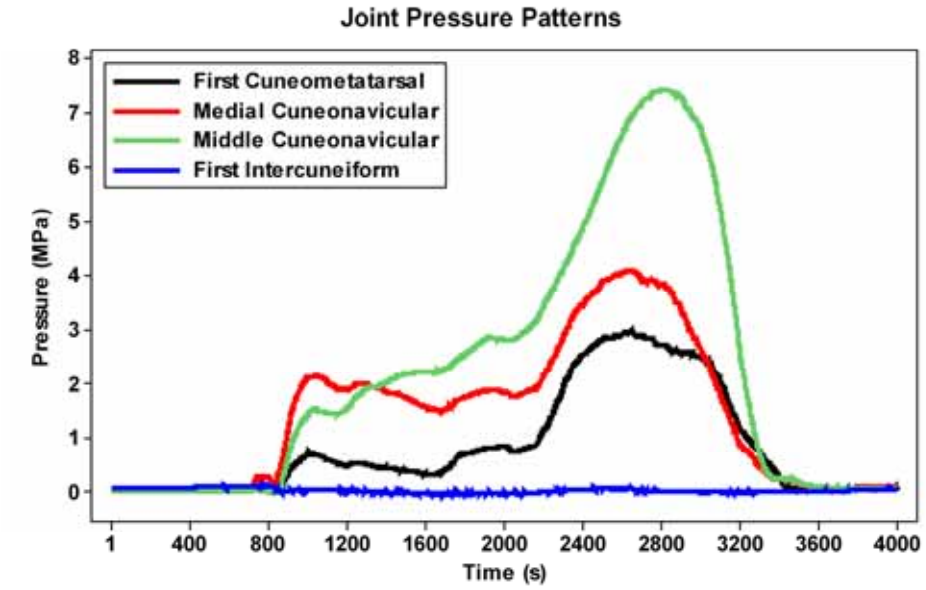

Figure 2.11. Joint pressure patterns at four medial joints of the midfoot during walking simulation.

2.6 Discussion

The new control software for the UMS has successfully demonstrated the ability to perform walking simulations with cadaver feet in order to investigate orthopedic research questions. The ability to simulate and vary specific parameters of physiological and pathological conditions would give physicians boundless opportunities for pre-clinical studies. This is not limited to walking studies either. Provided the motion that is desired to be replicated in within the range of motion of the robot, the activities of daily living that can be simulated are numerous. In addition, the communication function for external measurement software would allow the researchers to use all different types of internal or external sensors to simultaneously assess physiological conditions.

A customized error handling function was built to prevent bugs from stalling the operation of the UMS during the experiment. The main limitation of this control software was the optimization process. The fuzzy logic controllers were empirically determined algorithms and gains that were very effective on the vertical GRF axis, somewhat effective on the anterior GRF and COP, and not effective on the medial GRF or COP. Additionally, the algorithms provided non-unique solutions to the optimization given that there were 6 inputs (GRF) and 11 outputs (6 DOF kinematics and 5 tendon actuators).

2.7 References

Nester, C.J., Liu, A.M., Ward, E., Howard, D., Cocheba, J., Derrick, T., Patterson, P., 2007. In vitro studt of foot kinematics using a dynamic walking cadaver medel. Journal of Biomechanics 40 (9), 1927-1937.

Hurschler, C., Emmerich, J., Wülker, N., 2003. In vitro simulation of stance phase gait

part I: Model verification. Foot & Ankle International 24 (8), 614-622.

Kim, K., Kitaoka, H.B., Luo, Z., Ozeki, S., Berglund, L.J., Kaufman, K.R., An, K., 2001. In vitro simulation of the stance phase in human gait. Journal of Musculoskeletal Research 5 (2), 113-121.

Sharkey, N.A., Hamel, A.J., 1998. A dynamic cadaver model of the stance phase of gait: performance characteristics and kinetic validation. Clinical Biomechanics 13 (6), 420-433.

Aubin, P.M., Cowley M.S., Ledoux W.R., 2008, Gait simulation via a 6-DOF parallel robot with iterative learning control. IEEE transaction on biomedical engineering 55 (3), 1237-1240.

Perry, J., 1992. Gait Analysis – Normal and Pathological Function. New Jersey, Slack Incorporated, pp. 55-60.

2.8 Acknowledgement

Funding was provided through a NASA grant (NNJ05HF55G) and NIAMS Core Center Grant (#1P30AR-050953). Brandy Wozniak, Lawrence D. Noble, and Drs. Antonie J. van den Bogert and Peter R. Cavanagh provided valuable assistance.

CHAPTER III

ASSESSMENT OF THE EFFECTS OF DIABETES ON JOINT PRESSURES OF THE MIDFOOT USING A ROBOTIC GAIT SIMULATOR

Dong Gil Lee and Brian L. Davis

Foot & Ankle International, submitted.

3.1 Preface

Charcot Neuroarthropathy (CN) is one of the most serious diabetic foot complications that result in progressive arch collapsing and permanent foot deformity. Both clinical physicians and scientists have been undergoing a tremendous endeavor to learn about the etiological causes of diabetic foot problems; from cell property to subject's characteristics analysis. However, the exact etiology is still unidentified. A number of *in vivo* studies suggested that diabetic patients have stiff tissue and rigid structure and demonstrated that these differences lead to further complications of their feet. This study focused on a biomechanical point of view to assess of peak joint pressure difference between diabetic and non-diabetic cadaver feet during simulated walking.

3.2 Abstract

As the diabetic population increases, foot problems become more common and difficult to manage. One of the more serious diabetic complications is Charcot Neuroarthropathy (CN), a progressive joint disease that results in arch collapse and permanent foot deformity. However, very little is known about the etiology of CN. From a mechanical standpoint, it is likely that there is a "vicious circle" in terms of (i) arch collapse causing increased joint pressures of the midfoot, and (ii) increased joint contact pressures exacerbating the collapse of bones of the midfoot. This study focused on assessment of peak joint pressure difference between diabetic and non-diabetic cadaver feet during simulated walking. We hypothesized that joint pressures are higher for diabetics than normal population. Sixteen cadaver foot specimens (eight control and eight diabetic specimens) were used in this study. Human gait at 25% of typical walking speed (averaged stance duration of 3.2s) was simulated by a custom-designed Universal Musculoskeletal Simulator. Four medial joint pressures of the midfoot (the first cuneometatarsal, medial cuneonavicular, middle cuneonavicular, and first intercuneiform) were measured dynamically during full stance ($p=0.1437$, $p=0.1654$, $p=0.0089$, and $p=0.9789$ respectively). Across all four tested joints, the diabetic cadaver specimens had, on average, 46% higher peak pressures than the control cadaver feet during the simulated stance phase. This finding suggests that diabetic patients could be predisposed to arch collapse even before there are visible signs of bone or joint abnormalities.

3.3 Introduction

As the diabetic population gets larger, diabetic foot problems are becoming increasingly serious (Davis *et al.*, 2004; Shojaie Fard *et al.*, 2008). Despite extensive efforts on the part of physicians and scientists to understand Charcot Neuroarthropathy (CN), the exact etiology is still unidentified. This progressive joint disease results in permanent foot deformity (Caputo *et al.*, 1998). Over seventy percent of CN cases have been found at the first ray and midfoot area; areas which are most vulnerable to distorted architecture and foot arch collapse with progression of the disease (Trepman *et al.*, 2005; Rajbhandari *et al.*, 2002). A number of published research papers have proposed possible causes regarding diabetic foot problems. For example, it has been reported that people with diabetes have increased thickness in plantar fascia and Achilles tendon compared to control subjects (Giacomozzi, 2005). This biological change involves the inverse relationship between the thickness of plantar fascia and metatarsal-phalangeal (MTP) joint mobility (D'Ambrogi *et al.*, 2003). In addition, it has been shown that patients with diabetes have limited foot joint mobility compared with non-diabetic subjects, and this can result in higher plantar pressure in the diabetic patients during walking (Viswanathan *et al.*, 2003). Similarly, it has been found that there is an inverse correlation between the mobility of the MTP joint and the pressure-time integral under the forefoot in the diabetic patients (Zimmy *et al.*, 2004). Because of these biological and mechanical changes in tissues in patients with diabetes, it has been proposed that limited foot joint mobility could play an important role in arch collapse (Lee *et al.*, 2003).

Not surprisingly, most in vivo studies have focused on parameters measured external to the foot for ethical issues. For this reason, many robotic systems have been

developed and given validated ability to simulate human walking motion using cadaver feet (Nester *et al.*, 2007; Hurschler *et al.*, 2003; Kim *et al.*, 2001; Sharkey *et al.*, 1998).

The purpose of this study was to examine joint pressure difference of the midfoot between normal and diabetic cadaver feet during simulated gait with a robotic system; the Universal Musculoskeletal Simulator (UMS). We hypothesized that joint pressures of the midfoot are higher for diabetics than the normal population due to increased stiffness of soft tissues and limited range of joint motion.

3.4 Materials and Methods

Specimen Information and preparation

A total of sixteen cadaver foot specimens (eight control and eight diabetic specimens) were used in this study. The foot specimens were obtained from eight male and eight female donors whose average age was 80.0 ± 8.0 years old. In order to mount cadaver foot specimens on the UMS, all soft tissues, except tendons, were removed above one inch from the center of the ankle joint in order to fasten the exposed tibia and fibular into the fixture using wood's metal®. All specimens maintained a close to natural wet condition during the experiment by putting on Vaseline® and distilled water on the dorsum of the foot. Characteristics of the two specimen groups are shown in (Table 3.1).

Table 3.1. Variables in two specimen groups.

	Control Group (n=8)	**Diabetic Group (n=8)**
Average Simulated Body Weight (Kg)	44.7 ± 7.9	40.7 ± 12.1
Average Age (Year)	79.3 ± 7.8	80.7 ± 8.6
Gender (Male/Female)	5M / 3F	3M / 5F
Foot Side (Right/Left)	5R / 3L	5R / 3L
Average Foot Length (cm)	24.0 ± 1.8	23.3 ± 0.9
Average Foot Width (cm)	8.6 ± 0.9	8.5 ± 0.6
Average Arch Height (cm)	2.4 ± 0.8	2.8 ± 0.6

* Confidence level for mean 95%

Experimental Set-up and Measurement Protocol

In order to provide desired kinematic and kinetic data for the UMS, a number of walking patterns and ground reaction forces were captured simultaneously from a volunteer using a motion capture system (Eagle, Motion Analysis Corporation, Santa Rosa, California) with a force plate system (OR 6-7, AMTI, Watertown, Massachusetts) in a gait laboratory. The subject walked about 5m at an average walking speed of 1.5 m/s along a straight line. Eleven markers were attached on the subject's right leg to determine anatomical joint coordinate system, three dimensional rotation, and translation changes between the moving tibia and stationary ground origin during walking (Table 3.2). In addition, five markers were attached on the force plate to assess the three dimensional tibia orientation changes about this ground origin during the walking. The anatomical coordinate system followed the International Society of Biomechanics standards (ISB recommendation, 2002). To minimize data acquisition delay and timing difference between the motion capture system and ground mounted force plate system, both of these

systems acquired the data at the maximum sampling rate, 60 Hz and 240 Hz respectively. A desired walking pattern and ground reaction force were generated by averaging the best 10 walking data among many trials.

Table 3.2. Marker set for measuring subject's walking motion.

Purpose	Location of Markers
Defining joint centers Defining segment reference frames	Lateral epicondyle of knee Medial epicondyle Lateral malleolus Medial malleolus
Defining tibia motion during walking	Tibial tuberosity Head of fibula Anterior-medial tibia Lateral fibula
For ankle joint motion	Back of the heel Lateral heel Head of fifth metatarsal

The UMS consists of a six-degrees-of-freedom parallel robot (R-2000, Parallel Robotic System Corporation, Hampton, New Hampshire), a force plate (4060A, Bertec, Columbus, Ohio), a microscribe (G2L, Immersion Corporation, San Jose, California), a rotary type Achilles tendon actuator (BSM80N-275AE servomotor, Baldor, Forth Smith, Arizona / CSG-40-50 harmonic drive, Harmonic Drive Systems, Hauppauge, New York), four linear type tendon actuators (SM233A servomotors and ET-50 series actuators, Parker, Rohnert Park, California), and a control software coded in LabVIEW (LabVIEW 8.2, National Instrument, Austin, Texas) (Figure 3.1). In order to recreate walking motion, the tibia was fixed on the UMS frame and the force plate was mounted vertically on the top of the parallel robot's platform to create inverted ground-tibia motion (Figure 3.2).

This unique idea provided two major benefits. First, it did not require rotating the entire tendon actuators system in accordance with the tibia motion during walking simulation. This was made possible because the tibia was fixed on the UMS frame. Second, because the parallel robot's range of motion has a cylinder-like-shape, the inverted walking motion, mostly ankle joint centered rotation, simulates full stance. In addition, the force plate was shifted by 75 mm away from the center of the platform to get the maximized range of motion in order to simulate the inverted walking motion. The microscribe provided 3-D information (x, y, z) about the center of the robot's platform, the location and posture of the vertically mounted force plate, and the location and size of the mounted specimen. Based on these measured coordinates, the control software created 4×4 transformation matrixes for the defined coordinate systems of the UMS. In addition, the control software generated the parallel robot's trajectories in accordance with measured foot length and width using the microscribe data from normalized desired trajectories. Five tendon actuators provided muscle forces during simulated walking. Muscle forces were generated by the tendon actuators (the Achilles, tibialis posterior, tibialis anterior, flexor hallucis longus, and peroneus longus). Initial muscle force patterns were generated manually based on published EMG reference graphs (Perry, 1992). Control software was developed to setup all hardware components, to control the parallel robot and the tendon actuators, and to collect data. The data were collected from the vertically mounted force plate and the tendon actuator's load cells. Control software acquired all force data at 1000 Hz sampling rate by a PCI-6034E DAQ board (National Instruments, Austin, Texas).

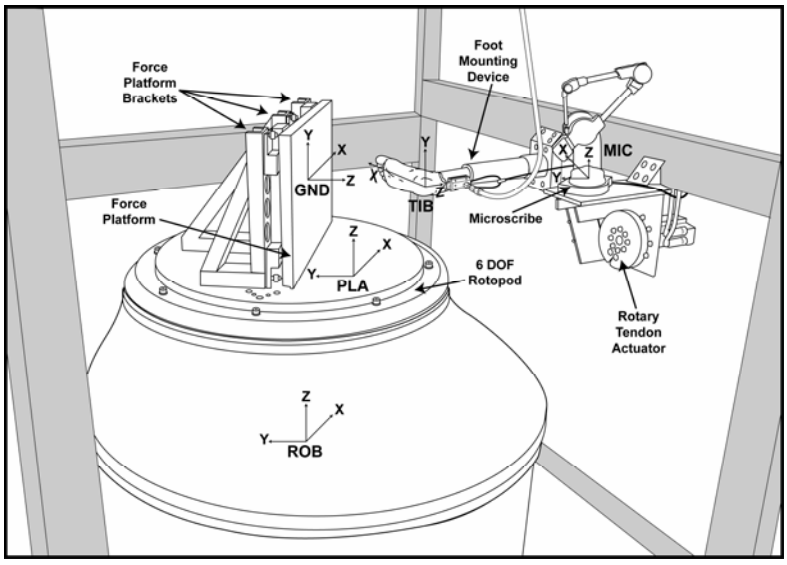

Figure 3.1. Illustration of the Universal Musculoskeletal Simulator.

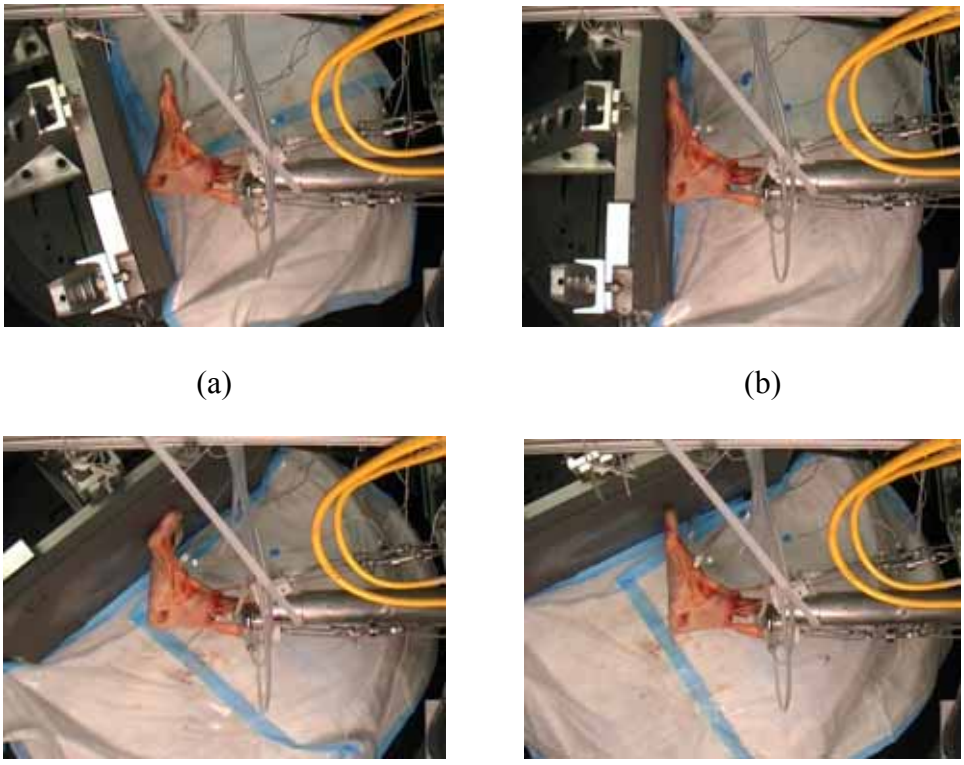

(a) (b)

(c) (d)

Figure 3.2. Inverted walking motion was created by the UMS with cadaver specimens.

For joint pressure measurement, thin film pressure sensors (A201, Tekscan, South Boston, Massachusetts), a customized signal conditioner, a multiplexer with Butterworth low pass filter (SCXI-1000 / 1143 / 1305, National Instruments, Austin, Texas), a PCI-6229 DAQ board (National Instruments, Austin, Texas), and Labview measurement software were used. The performance of the thin film pressure sensor was verified by published research papers (Ferguson-Pell *et al.*, 2000). For foot joint pressure measurement, the thin film pressure sensors were calibrated dynamically. The cut-off frequency for the Butterworth low pass filter was set at 200Hz in order to prevent signal delay.

Four medial joints of the midfoot (the first cuneometatarsal, medial cuneonavicular, middle cuneovavicular, and first intercuneiform) were chosen for this study due to the functional importance of the first ray and structural importance of the second cuneiform (Cornwall et al., 2004; Makwana, 2005) (Figure 3.3). Pressure sensors were carefully inserted into each joint and attached on the bone surface directly using super glue to minimize any other mechanical effect.

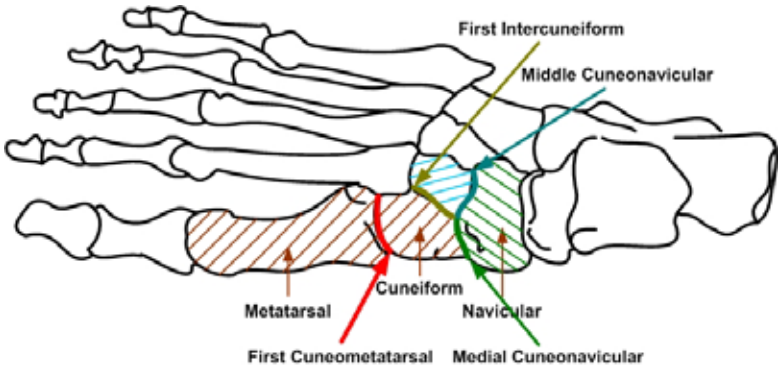

Figure 3.3. Locations of four medial joints of the midfoot.

Full stance of human gait at ¼ of the speed (averaged stance duration of 3.2s) with 66.7% body weight was simulated by the UMS. Limitations of the simulated speed and body weight were properly matched to mechanical limitations of the UMS and range limitation of the pressure sensor respectively.

Statistical Analysis

Peak joint pressure difference regarding effect of diabetes at each joint between two experimental groups was evaluated with the repeated measures method using SAS (version 9.2, SAS Institute Inc, Cary, North Carolina).

3.5 Results

Peak pressure range at various joints of the midfoot differed substantially - in particular, the highest peak joint pressures were found at the middle cuneonavicular in the most of specimens (Table 3.3). Measurement of peak joint pressure at the first cuneometatarsal showed a higher mean value in diabetic specimens than that of the control. Evaluation of the medial cuneonavicular proved a considerable difference in peak joint pressure value between the two groups. Study of middle cuneonavicular demonstrated a significant difference in peak joint pressure of the two groups (Figure 3.4). The first intercuneiform had similar peak joint pressure ranges between the two groups. Across all four tested joints, the diabetic cadaver feet had, on average, 46% higher peak pressures than the control cadaver feet during the simulated stance phase.

Table 3.3. Analysis for four peak joint pressures of the midfoot.

Location	Group	Least Square Mean	Standard Error
First Cuneometatarsal	Control	3.3314	1.0820
(p=0.1437)	Diabetic	5.7130	1.0825
Medial Cuneonavicular	Control	2.7635	1.0947
(p=0.1654)	Diabetic	4.9771	1.0238
Middle Cuneonavicular	Control	4.3012	0.9354
(**p=0.0089**)	Diabetic	8.2893	0.8657
First Intercuneoform	Control	1.2046	0.3895
(p=0.9789)	Diabetic	1.2195	0.3898

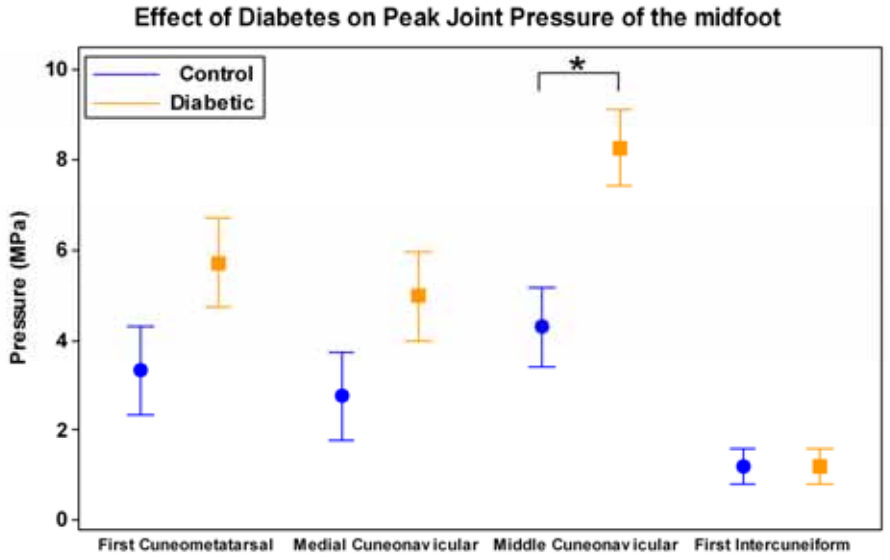

Figure 3.4. The effect of diabetes on peak pressures demonstrated a statistical significance at the middle cuneonavicular (p=0.0089).

3.6 Discussion

Robotic gait simulation using cadaver specimens allows investigators to study the pathomechanics associated with various disorders. Of relevance to the current study is the fact that a universal musculoskeletal simulator permits measurements to be made internally, while external factors such as ground reaction forces, tendon tensions and

ankle angles are tightly controlled.

While there were some limitations in terms of creating high-fidelity ground reaction forces at heelstrike, the primary variable of interest, peak joint pressure, occurred during the push-off phase. It was therefore less influenced by heel strike events. Furthermore, while pronated or supinated walking patterns could affect midfoot joint pressures, these patterns were not of primary interest in this study. Published research articles have demonstrated different walking patterns in people with diabetes compared to control subjects (Mueller *et al.*, 1994). This suggests that future work may need to focus on the effects of various walking patterns. There is also a need to determine methods for simulating the effects of intrinsic muscle actions.

The wide distributions of foot joint pressure are most likely due to anatomical differences among various specimens. In addition, there could be some variability induced by removing the joint capsule and ligamentous tissue during the pressure sensor insertion process.

Despite these limitations, the dramatic increase in joint pressures of the midfoot found in diabetic specimens could be due to (i) increased stiffness in diabetic soft tissue, (ii) limited range of the foot joints motion, or both in combination. These findings suggest that people with diabetes have higher mechanical stresses on their joints of the midfoot than control subjects during daily activities. Also, the application of repetitive high joint pressures in diabetic feet may result in acceleration of joint problems. This result suggests that patients with diabetes are predisposed to mechanical alterations in the arch of their feet, even without visible signs of midfoot collapse.

3.7 References

Davis, B.L., Kuznicki, J., Praveen, S.S., Sferra, J.J., 2004. Lower-extremity amputations in patients with diabetes: pre- and post-surgical decisions related to successful rehabilitation. Diabetes Metabolism Research and Reviews 20 (Suppl 1), S45-S50.

Shojaie Fard, A., Esmaelzadeh, M., Larijani, B., 2008. Assessment and treatment of diabetic foot ulcer. International Journal of Clinical Practice 61 (11), 1931-1938.

Caputo, G.M., Ulbrecht, J., Cavanagh, P.R., 1998. The charcot foot in diabetes: six key points. American Family Physician 57 (11), 2705-2710.

Trepman, E., Nihal, A., Pinzur, M.S., 2005. Charcot neuroarthropathy of the foot and ankle. Foot & Ankle International 26 (1), 46-63.

Rajbhandari, S.M., Jenkins, R.C., Davies, C., Tesfaye, S., 2002. Charcot neuroarthropathy in diabetes mellitus. Diabetologia 45 (8), 1085-1096.

Giacomozzi, C., D'Ambrogi, E., Uccioli, L., Macellari, V., 2005. Does the thickening of Achilles tendon and plantar fascia contribute to the alteration of diabetic foot loading? Clinical Biomechanics 20 (5), 532-539.

D'Ambrogi, E., Macellari, V.M., Giurato, L., Caselli, A., D'Agostino, M.A., Ucciolo, L., Giacomozzi, C., 2003. Contribution of plantar fascia to the increased forefoot pressures in diabetic patients. Diabetes Care 26 (5), 1525-1529.

Viswanathan, V., Snehalatha, C., Sivagami, M., Seena, R., Ramachandran, A., 2003. Association of limited joint mobility and high plantar pressure in diabetic foot ulceration in Asian Indians. Diabetes Research and Clinical Practice 60 (1), 57-61.

Zimny, S., Schatz, H., Pfohl, M., 2004. The role of limited joint mobility in diabetic patients with an at-risk foot. Diabetes Care 27 (4), 942-946.

Lee, L., Blume, P.A., Sumpio, B., 2003. Charcot joint disease in diabetes mellitus. Annals of Vascular Surgery 17 (5), 571-580.

Nester, C.J., Liu, A.M., Ward, E., Howard, D., Cocheba, J., Derrick, T., Patterson, P., 2007. In vitro studt of foot kinematics using a dynamic walking cadaver medel. Journal of Biomechanics 40 (9), 1927-1937.

Hurschler, C., Emmerich, J., Wülker, N., 2003. In vitro simulation of stance phase gait part I: Model verification. Foot & Ankle International 24 (8), 614-622.

Kim, K., Kitaoka, H.B., Luo, Z., Ozeki, S., Berglund, L.J., Kaufman, K.R., An, K., 2001. In vitro simulation of the stance phase in human gait. Journal of Musculoskeletal Research 5 (2), 113-121.

Sharkey, N.A., Hamel, A.J., 1998. A dynamic cadaver model of the stance phase of gait: performance characteristics and kinetic validation. Clinical Biomechanics 13 (6), 420-433.

ISB recommendation on definitions of joint coordinate system of carious joints for the reporting of human joint motion - part I: ankle, hip, and spine. 2002. Journal of Biomechanics 35 (4), 543-548.

Perry, J., 1992. Gait Analysis – Normal and Pathological Function. New Jersey, Slack Incorporated, pp. 55-60.

Ferguson-Pell, M., Hagisawa, S., Bain, D., 2000. Evaluation of a sensor for low interface pressure applications. Medical Engineering & Physics 22 (9), 657-663.

Cornwall, M.W., Fishco, W.D., McPoil, T.G., Lane, C.R., O'Donnell, D., Hunt, L., 2004. Reliability and validity of clinically assessing first-ray mobility of the foot. Journal of American Podiatric Medical Association 94 (5), 470-476.

Makwana, N.K., 2005. (iii) Tarsometatarsal injuries-Lisfranc injuries. Current Orthopaedics 19 (2), 108-118.

Mueller, M.J., Minor, S.D., Sahrmann, S.A., Schaaf, J.A., Strube, M.J., 1994. Differences in the gait characteristics of patients with diabetes and peripheral neuropathy compared with age-matched controls. Physical Therapy 74 (4), 299-313.

3.8 Acknowledgement

Funding was provided through a NASA grant (NNJ05HF55G) and NIAMS Core Center Grant (#1P30AR-050953). Brandy Wozniak, Lawrence D. Noble, Robb W. Colbrunn and Drs. Antonie J. van den Bogert and Peter R. Cavanagh provided valuable assistance.

CHAPTER IV

DETERMINATION OF JOINT PRESSURES OF THE MIDFOOT USING A ROBOTIC GAIT SIMULATOR: DIABETIC DIFFERENCES AND ARTIFICIALLY INDUCED FLATFOOT DEFORMITIES

Dong Gil Lee and Brian L. Davis

Journal of Mechanics in Medicine and Biology, submitted.

4.1 Preface

A number of studies suggested there are possible factors causing mechanical impacts and foot injuries that are associated with the arch height. A flatfoot has generally been considered one of a troubled foot condition. However, it is unclear whether there is or is not a direct relationship between arch height and injury risks in a human foot. The purpose of this study was to examine the difference in joint pressure of the midfoot during simulated arch collapse. This study was based on the idea that a foot collapse could be simulated by an altered ligamentous arch support. In addition, we compared joint pressures between diabetic and control cadaver specimens to show evidence of higher joint pressures in the diabetic group during the arch collapse simulation.

4.2 Abstract

The purpose of this study was to examine the difference in midfoot joint pressures during simulated arch collapse in normal and diabetic groups. This study was based on the idea that diminished ligamentous arch support could simulate foot collapse. We hypothesized that arch collapse could result in higher joint pressures of the midfoot during walking simulations. In addition, it was hypothesized that diabetic cadaver specimens would show evidence of higher joint pressures during the arch collapse than control specimens. Sixteen cadaver feet were tested with a robotic system that simulates the full stance of human gait at ¼ of the normal speed with 66.7% body weight. Foot arch collapse was simulated by transecting both the plantar aponeurosis and spring ligament. Four medial joints of the midfoot (the first cuneometatarsal, medial cuneonavicular, middle cuneonavicular, and first intercuneiform) were chosen for this study.

Transecting ligaments resulted in statistically significant increases of 13%, 17%, and 16% in peak joint pressures at the first cuneometatarsal, middle cuneonavicular, and first intercuneiform respectively. Across all of the tested joints and conditions, the diabetic cadaver feet had, on average, 54% higher peak pressures than the control cadaver feet during the stance phase.

4.3 Introduction

Human feet dynamically interact between the body and ground during walking. A foot arch, which is shaped like a multi-segmented curvature, acts as a spring to make walking and running more effective (Ker *et al.*, 1987). It is well known that ligaments in

the foot, such as plantar aponeurosis, plantar ligaments, and spring ligaments, are important components contributing to this spring-like property of the arch (Huang *et al.*, 1993). In addition, separate bones in the arch are bound together on the lower concave side by the ligaments. The basic function of the ligaments is a tie-rod, which takes tension and eliminates bending while bearing weight. According to a more dynamic "windlass" foot model, the plantar aponeurosis works as a tension band, changing the arch height and bone's orientation responsively for effective walking strides (Bolgla *et al.*, 2004). This theoretical model has been verified by investigating changes in the arch height during walking (Cashmere *et al.*, 1999). The implication is that losing ligamentous support could cause faulty foot mechanics during walking.

It is well known that repeated loading is highly associated with foot injuries and that altered foot structure can affect lower extremity injury (Macintyre *et al.*, 2000; Rudzki 1997; Cowan *et al.*, 1993). People with a higher or lower foot arch are more likely to develop soft tissue damages, such as plantar fasciitis (Bolgla *et al.*, 2004). *In vivo* studies found different patterns in ground reaction forces during running for individuals who have different arch heights (Nachbauer *et al.*, 1992). Moreover, the ground reaction forces have been evaluated to extract meaningful factors in diagnosing medical problems caused by flat foot (Bertani *et al.*, 1999). These studies suggested there are possible factors causing mechanical impacts and foot injuries that are associated with the arch height.

To further examine the walking mechanics, experimental studies have been performed to determine the structural function of the ligaments. Ker *et al.* (1987) and Haung *et al.* (1993) demonstrated that the ligaments are important in maintaining the

shape of the foot arch by conducting cadaver studies. Kitaoka *et al.* (1997) showed that losing individual ligament in the foot affects specific midfoot bone orientations. Furthermore, it has been suggested that the structural alteration of feet is correlated with mechanical differences (Arangio *et al.*, 1997). These studies clearly demonstrated that one of the functions of the ligaments is providing support for the foot arch.

Walking mechanics are very significant in diabetic patients. It has been observed that muscle weakness and joint stiffness often occur in the foot of neuropathic diabetic patients (van Schie *et al.*, 2004; Viswanathan *et al.*, 2003). Muscle weakness and joint stiffness are responsible for the alteration of motions, which could result in a distorted architecture of the foot and eventually lead to serious diabetic foot complications. One of the most serious diabetic foot complications is Charcot foot (Caputo *et al.*, 1998). Generally, the Charcot foot engages a sequential series of events: bone and joint fracture to fracture resorption, which leads to bone formation remodeling (Guyton *et al.*, 2001). The Charcot foot has been found primarily in the tarsal joints (60%), metatarsophalangeal joints (31%), and the ankle joint (9%) (Wolfe *et al.*, 1991). Limited range of motion in the Charcot foot moves the plantar load anteriorly (Lee *et al.*, 2003). However, it is not well known if the altered joint configurations result in the increased joint stress during gait. If so, there could be a "vicious cycle" in which the joint stress increases as the arch height diminishes, which may then lead to further increases in the joint stress.

The purpose of this study was to examine joint pressure differences of the midfoot during an induced arch collapsing with a robotic gait simulator. This study focused on the relative importance of the ligaments and bony structure in determining the

arch height and joint stresses. We hypothesized that arch collapse could result in higher joint pressures of the midfoot during walking. In addition, it was hypothesized that diabetic cadaver specimens would show evidence of higher joint pressures during arch collapse than control specimens.

4.4 Research methods and design

Generation of Walking Model, Experimental Set-up, and Specimen Information

Generation of walking model, experimental set-up, and specimen information were described in Chapter 3.4.

Measurement Protocol

The plantar aponeurosis and spring ligament were transected in two ways to simulate two possible situations of the arch collapse effect: the plantar aponeurosis first, then spring ligament, and *vice versa*. Three anatomical points of medial foot, the metatarsal head, navicular, and calcaneus, were measured in order to define the arch height under the loading at each condition using the microscribe. Four medial joints of the midfoot (the first cuneometatarsal, medial cuneonavicular, middle cuneonavicular, and first intercuneiform) were specifically chosen for this study due to the functional importance of the first ray and the structural importance of the second cuneiform (Cornwall *et al.*, 2004; Makwana, 2005). Pressure sensors were carefully inserted into each joint and attached on the bone surface directly using super glue to minimize any other mechanical effect.

Full stance of human gait at ¼ of the speed (averaged stance duration of 3.2s) with 66.7% body weight was simulated by the UMS. The limitations of the simulated

speed and body weight were properly matched to the mechanical limitations of the UMS and the range limitation of the pressure sensors respectively.

Statistical Analysis

The relationship between peak joint pressure change and arch height change was analyzed by regression and correlation analysis. The effect of transecting ligaments and diabetes on the peak joint pressure was assessed by the methods of repeated measures mixed model. All pairwise comparisons of least square means were made using the Tukey-Kramer adjustment for multiple comparisons. Minitab (version 15, Minitab Inc, State College, Pennsylvania) and SAS (version 9.2, SAS Institute Inc, Cary, North Carolina) were used to perform the statistical analysis.

4.5 Results

Effect of losing ligaments and diabetes on joint pressure

Transecting ligaments [Specimen Condition in the Tables (1: intact), (2: transecting spring ligament), (3: transecting plantar aponeurosis), and (4: transecting both ligaments)] influenced statistically significant value changes on the peak pressure at the first cuneometatarsal, middle cuneonavicular, and first intercuneiform joints during walking simulation ($p=0.0091$, $p<0.0001$, and $p=0.0086$ respectively). Analysis of the effect of diabetes [Diabetes in the Tables (0: non-diabetic) and (1: diabetic)] on the peak joint pressure showed that diabetes has a significant effect on the middle cuneonavicular joint during simulated arch collapse ($p=0.0119$). Across all tested joints, the diabetic group had a 54% higher peak joint pressure over all conditions. In addition, both combined effects affected peak pressure value in the middle cuneonavicular and first

intercuneiform joints (p=0.0128 and p<0.0001 respectively). Statistical analysis results were provided from Table 4.1 to Table 4.7 and from Figure 4.1 to figure 4.4.

Table 4.1. Analysis for the first cuneometatarsal joint.

Effect		P-Value	
Diabetes		0.0916	
Specimen Condition		**0.0091**	
Diabetes*Spec_Con		0.0911	
Effect	**Diabetes**	**Specimen Condition**	**Least Square Mean**
Diabetes	0	-	3.5141
Diabetes	1	-	5.9892
Specimen Condition	-	1	4.3131
Specimen Condition	-	2	4.6520
Specimen Condition	-	3	5.1404
Specimen Condition	-	4	4.9010
Diabetes*Spec_Con	0	1	3.0715
Diabetes*Spec_Con	0	2	3.7021
Diabetes*Spec_Con	0	3	3.4932
Diabetes*Spec_Con	0	4	3.7894
Diabetes*Spec_Con	1	1	5.5548
Diabetes*Spec_Con	1	2	5.6019
Diabetes*Spec_Con	1	3	6.7876
Diabetes*Spec_Con	1	4	6.0126

Table 4.2. Pairwise comparisons of significant least square mean differences for the first cuneometatarsal joint.

Effect	Diabetes	Spec_Con	Diabetes	Spec_Con	P-Value
Spec_Con	-	1	-	2	0.3948
Spec_Con	-	1	-	3	**0.0106**
Spec_Con	-	1	-	4	0.0535
Spec_Con	-	2	-	3	0.4135
Spec_Con	-	2	-	4	0.6803
Spec_Con	-	3	-	4	0.7922

Table 4.3. Analysis for the medial cuneonavicular joint.

Effect		P-Value	
Diabetes		0.0970	
Specimen Condition		0.1165	
Diabetes*Spec_Con		0.6627	
Effect	**Diabetes**	**Specimen Condition**	**Least Square Mean**
Diabetes	0	-	3.0295
Diabetes	1	-	5.4017
Specimen Condition	-	1	3.8458
Specimen Condition	-	2	3.8321
Specimen Condition	-	3	4.7504
Specimen Condition	-	4	4.4339
Diabetes*Spec_Con	0	1	2.7004
Diabetes*Spec_Con	0	2	2.9208
Diabetes*Spec_Con	0	3	3.2581
Diabetes*Spec_Con	0	4	3.2386
Diabetes*Spec_Con	1	1	4.9913
Diabetes*Spec_Con	1	2	4.7434
Diabetes*Spec_Con	1	3	6.2427
Diabetes*Spec_Con	1	4	5.6292

Table 4.4. Analysis for the middle cuneonavicular joint.

Effect		P-Value	
Diabetes		**0.0119**	
Specimen Condition		**<.0001**	
Diabetes*Spec_Con		**0.0128**	
Effect	**Diabetes**	**Specimen Condition**	**Least Square Mean**
Diabetes	0	-	5.8610
Diabetes	1	-	9.3231
Specimen Condition	-	1	6.7578
Specimen Condition	-	2	6.4923
Specimen Condition	-	3	9.1924
Specimen Condition	-	4	7.9256
Diabetes*Spec_Con	0	1	4.8340
Diabetes*Spec_Con	0	2	4.8469
Diabetes*Spec_Con	0	3	8.0915
Diabetes*Spec_Con	0	4	5.6716
Diabetes*Spec_Con	1	1	8.6817
Diabetes*Spec_Con	1	2	8.1378
Diabetes*Spec_Con	1	3	10.2933
Diabetes*Spec_Con	1	4	10.1797

Table 4.5. Pairwise comparisons of significant least square mean differences for the middle cuneonavicular joint.

Effect	Diabetes	Spec_Con	Diabetes	Spec_Con	P-Value
Spec_Con	-	1	-	2	0.8723
Spec_Con	-	1	-	3	**<.0001**
Spec_Con	-	1	-	4	**0.0055**
Spec_Con	-	2	-	3	**<.0001**
Spec_Con	-	2	-	4	**0.0006**
Spec_Con	-	3	-	4	**0.0120**
Diabetes*Spec_Con	0	1	0	2	1.0000
Diabetes*Spec_Con	0	1	0	3	**<.0001**
Diabetes*Spec_Con	0	1	0	4	0.5714
Diabetes*Spec_Con	0	1	1	1	**0.0416**
Diabetes*Spec_Con	0	1	1	2	0.1867
Diabetes*Spec_Con	0	1	1	3	**0.0010**
Diabetes*Spec_Con	0	1	1	4	**0.0013**
Diabetes*Spec_Con	0	2	0	3	**0.0003**
Diabetes*Spec_Con	0	2	0	4	0.5193
Diabetes*Spec_Con	0	2	1	1	**0.0483**
Diabetes*Spec_Con	0	2	1	2	0.1961
Diabetes*Spec_Con	0	2	1	3	**0.0011**
Diabetes*Spec_Con	0	2	1	4	**0.0014**
Diabetes*Spec_Con	0	3	0	4	**0.0026**
Diabetes*Spec_Con	0	3	1	1	0.9998
Diabetes*Spec_Con	0	3	1	2	1.0000
Diabetes*Spec_Con	0	3	1	3	0.7263
Diabetes*Spec_Con	0	3	1	4	0.7772
Diabetes*Spec_Con	0	4	1	1	0.2284
Diabetes*Spec_Con	0	4	1	2	0.5544
Diabetes*Spec_Con	0	4	1	3	**0.0087**
Diabetes*Spec_Con	0	4	1	4	**0.0104**
Diabetes*Spec_Con	1	1	1	2	0.9687
Diabetes*Spec_Con	1	1	1	3	**0.0100**
Diabetes*Spec_Con	1	1	1	4	**0.0297**
Diabetes*Spec_Con	1	2	1	3	**0.0266**
Diabetes*Spec_Con	1	2	1	4	**0.0053**
Diabetes*Spec_Con	1	3	1	4	1.0000

Table 4.6. Analysis for the first intercuneiform joint.

Effect	P-Value		
Diabetes	0.8671		
Specimen Condition	**0.0086**		
Diabetes*Spec_Con	**<.0001**		
Effect	**Diabetes**	**Specimen Condition**	**Least Square Mean**
Diabetes	0	-	1.1846
Diabetes	1	-	1.2777
Specimen Condition	-	1	1.1974
Specimen Condition	-	2	1.1904
Specimen Condition	-	3	1.1291
Specimen Condition	-	4	1.4078
Diabetes*Spec_Con	0	1	1.2208
Diabetes*Spec_Con	0	2	1.2336
Diabetes*Spec_Con	0	3	1.1837
Diabetes*Spec_Con	0	4	1.1003
Diabetes*Spec_Con	1	1	1.1739
Diabetes*Spec_Con	1	2	1.1472
Diabetes*Spec_Con	1	3	1.0745
Diabetes*Spec_Con	1	4	1.7153

Table 4.7. Pairwise comparisons of significant least square mean differences for the first intercuneiform joint.

Effect	Diabetes	Spec_Con	Diabetes	Spec_Con	P-Value
Spec_Con	-	1	-	2	0.9998
Spec_Con	-	1	-	3	0.8967
Spec_Con	-	1	-	4	0.0887
Spec_Con	-	2	-	3	0.9566
Spec_Con	-	2	-	4	0.0666
Spec_Con	-	3	-	4	**0.0278**
Diabetes*Spec_Con	0	1	0	2	1.0000
Diabetes*Spec_Con	0	1	0	3	1.0000
Diabetes*Spec_Con	0	1	0	4	0.9573
Diabetes*Spec_Con	0	1	1	1	1.0000
Diabetes*Spec_Con	0	1	1	2	1.0000
Diabetes*Spec_Con	0	1	1	3	1.0000
Diabetes*Spec_Con	0	1	1	4	0.9857
Diabetes*Spec_Con	0	2	0	3	1.0000
Diabetes*Spec_Con	0	2	0	4	0.9006
Diabetes*Spec_Con	0	2	1	1	1.0000
Diabetes*Spec_Con	0	2	1	2	1.0000
Diabetes*Spec_Con	0	2	1	3	1.0000
Diabetes*Spec_Con	0	2	1	4	0.9879
Diabetes*Spec_Con	0	3	0	4	0.9990
Diabetes*Spec_Con	0	3	1	1	1.0000
Diabetes*Spec_Con	0	3	1	2	1.0000
Diabetes*Spec_Con	0	3	1	3	1.0000
Diabetes*Spec_Con	0	3	1	4	0.9820
Diabetes*Spec_Con	0	4	1	1	1.0000
Diabetes*Spec_Con	0	4	1	2	1.0000
Diabetes*Spec_Con	0	4	1	3	1.0000
Diabetes*Spec_Con	0	4	1	4	0.9524
Diabetes*Spec_Con	1	1	1	2	1.0000
Diabetes*Spec_Con	1	1	1	3	0.9829
Diabetes*Spec_Con	1	1	1	4	**0.0002**
Diabetes*Spec_Con	1	2	1	3	0.9998
Diabetes*Spec_Con	1	2	1	4	**0.0006**
Diabetes*Spec_Con	1	3	1	4	**<.0001**

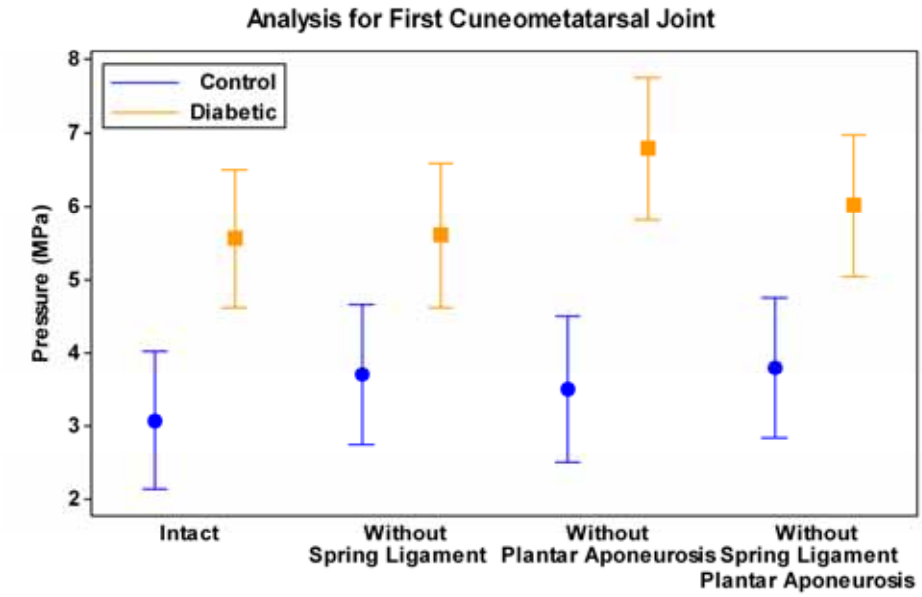

Figure 4.1. Analysis for the first cuneometatarsal joint.

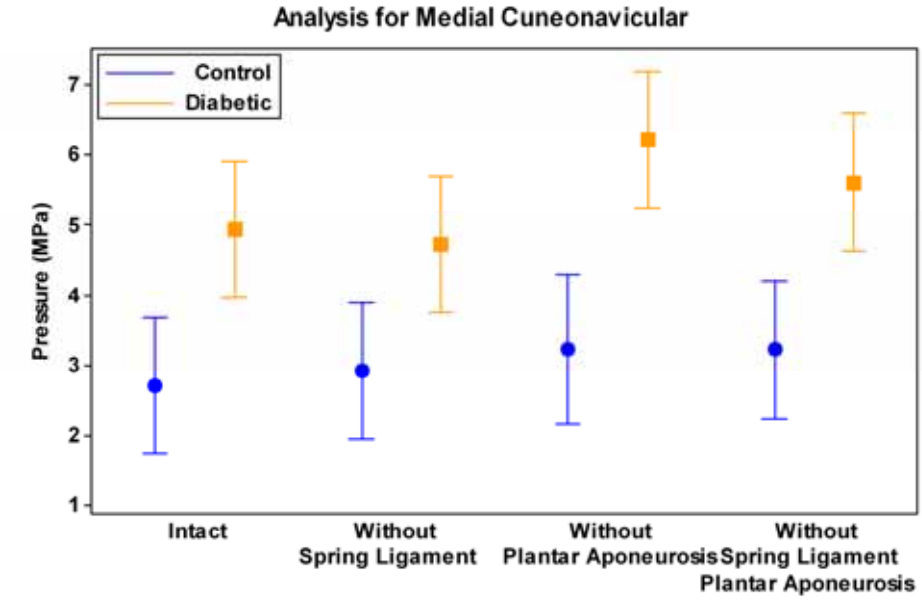

Figure 4.2. Analysis for the medial cuneonavicular joint.

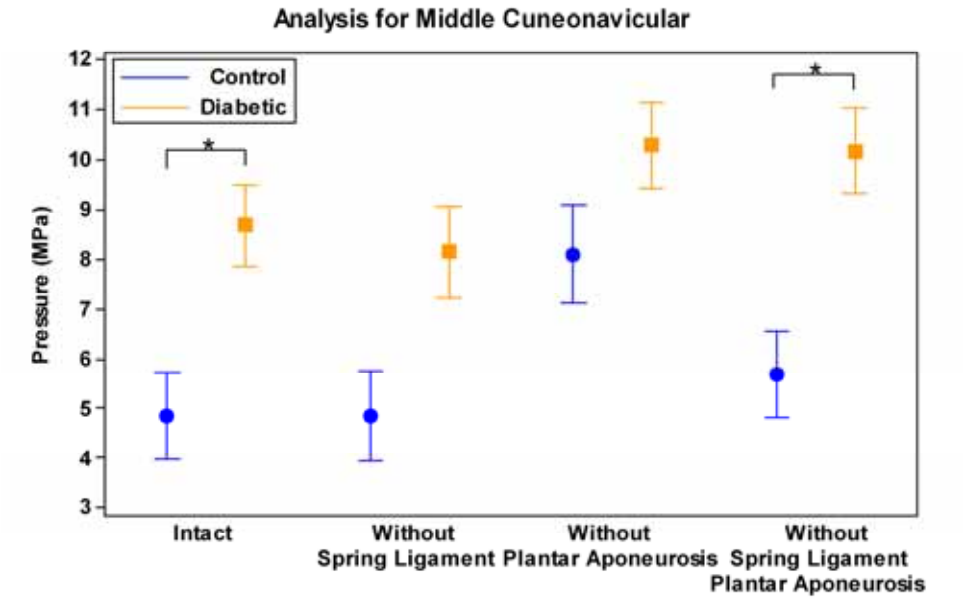

Figure 4.3. Analysis for the middle cuneonavicular joint.

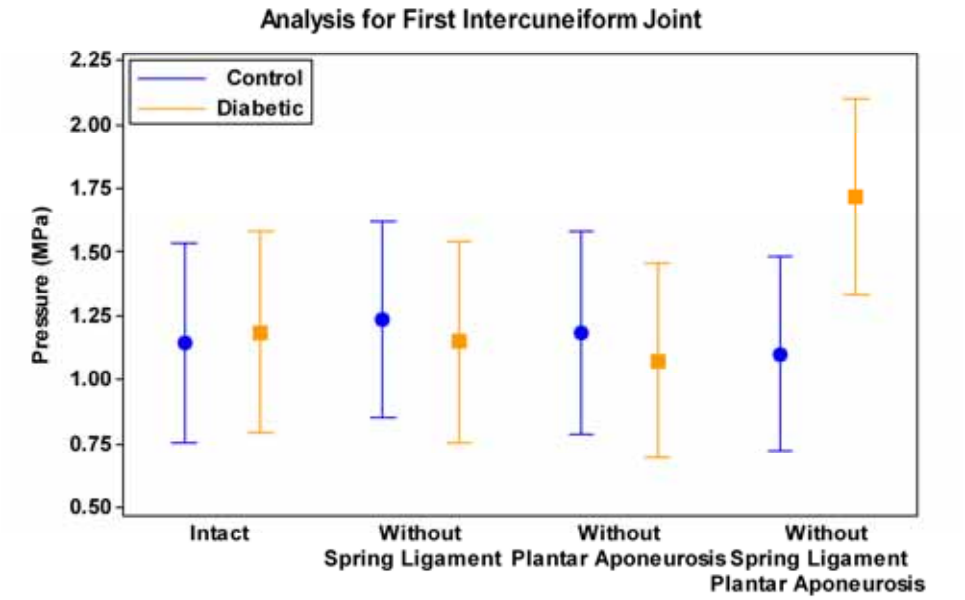

Figure 4.4. Analysis for the first intercuneiform joint.

Relationship between arch height and joint pressure

Peak joint pressure changes between two induced arch collapse ways showed different patterns. In the most of cases, correlation between peak joint pressure values and arch height values showed negative relationships (Figure 4.5 and Figure 4.6). In particular, when the plantar aponeurosis was transected first, correlation and R-square values demonstrated relatively substantial joint pressure joint pressure increases during arch collapse. Correlation and R-square values are presented in Table 4.8 and Table 4.9.

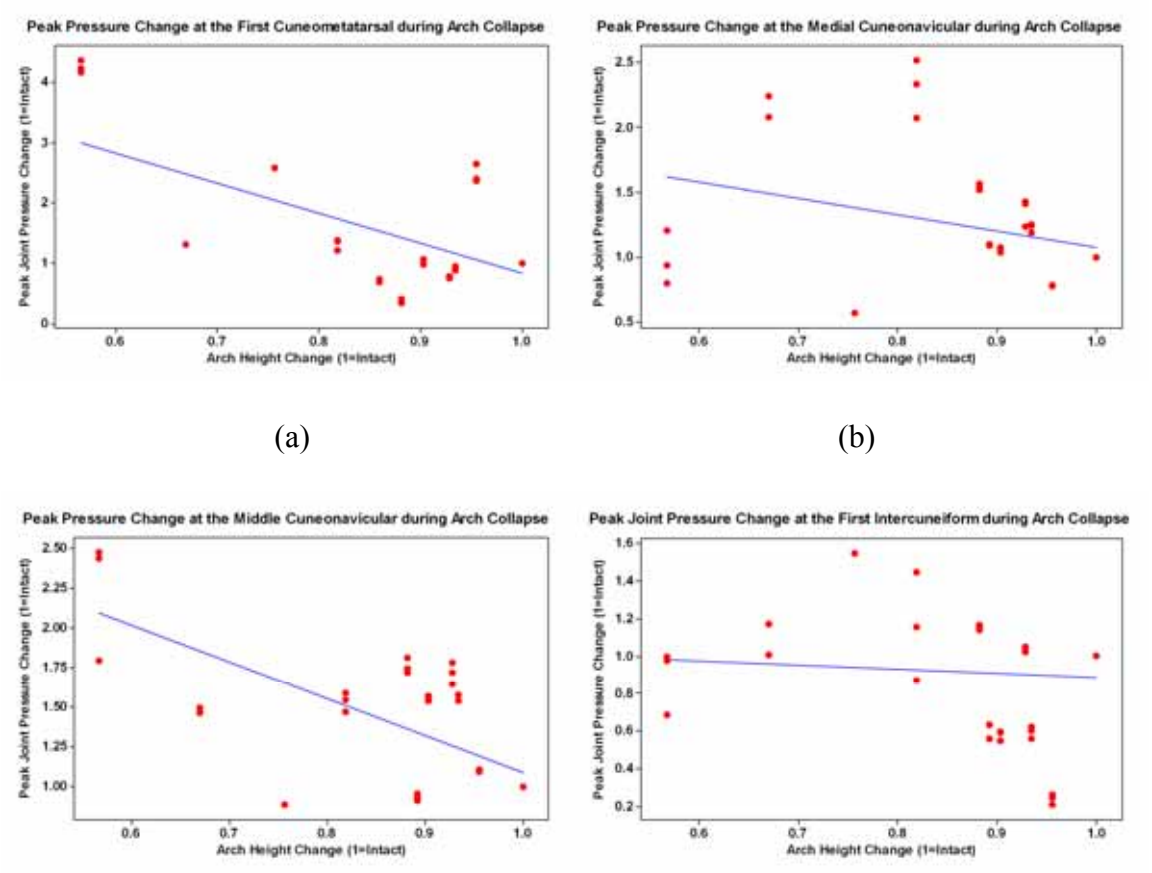

Figure 4.5. Peak joint pressures change during arch collapse when the plantar aponeurosis was transected first.

Table 4.8. Correlation and R-square values during arch collapse when plantar aponeurosis was transected first.

	Correlation Value	**R-Square Value**
First Cuneometatarsal	- 0.673	45.3%
Medial Cuneonavicular	- 0.370	13.7%
Middle Cuneonavicular	- 0.720	51.8%
First Intercuneiform	- 0.101	1%

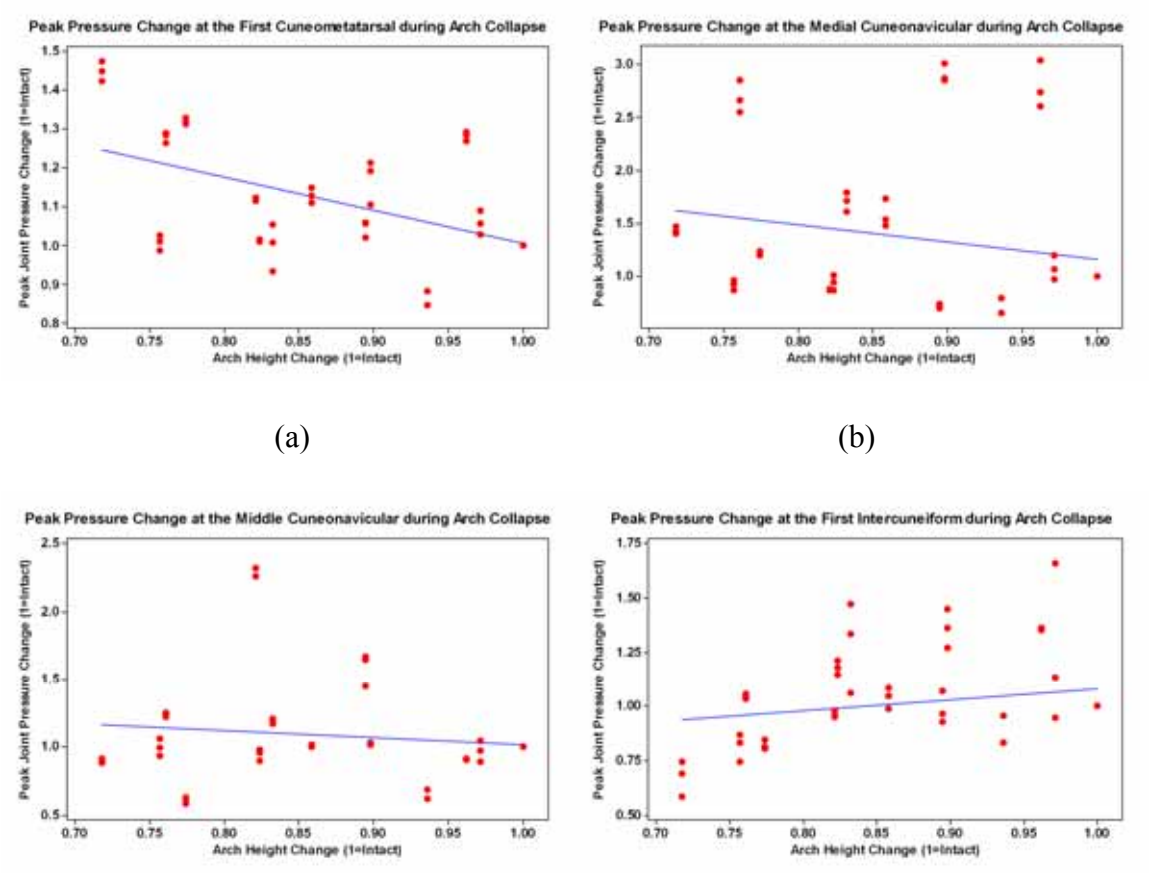

Figure 4.6. Peak joint pressures change during arch collapse when the spring ligament was transected first.

Table 4.9. Correlation and R-square values during arch collapse when the spring ligament was transected first.

	Correlation Value	**R-Square Value**
First Cuneometatarsal	- 0.614	37.7%
Medial Cuneonavicular	- 0.248	6.1%
Middle Cuneonavicular	- 0.155	2.4%
First Intercuneiform	0.257	6.6%

4.6 Discussion

Many studies have been conducted to find out the relationship between the arch height and foot disorders. It is well known that most people who have a low arch suffer from chronic foot pain. Conversely, there are two studies associating higher arches and the likelihood of developing foot injuries (Cowan *et al.*, 1993; Giladi *et al.*, 1985). A number of mechanical factors have a contributory effect on the foot injury development (Jones *et al.*, 1999). Collectively, these factors imply that the effect of the arch height on foot mechanics might be specific to an individual. As such, the anatomy and function of an innate flat foot could be different from an acquired flat foot.

In this study, we utilized a robotic gait simulator to provide possible answers for clinical questions regarding acquired flat foot. For example, it has been reported that patients who have undergone plantar fasciotomy are likely to develop midfoot pain, longitudinal arch syndrome, and gait pattern changes (Arangio *et al.*, 1997). Our findings of inverse correlations between the arch height and midfoot joint pressure could provide possible answers about the complications after plantar fasciotomy.

It is clear that the ligaments in the foot act as a bow-string that tightly support bone structures. We found that transecting ligaments increased mechanical stresses on the joints of the midfoot. However, the effect of transecting plantar aponeurosis was greater than the effect of transecting spring ligament. While transecting spring ligaments could cause collapse in the arch, other ligaments such as the plantar aponeurosis, still function as a windlass. This effect could dominate the mechanical stress on the foot during walking. In particular, it has been experimentally verified that the plantar aponeurosis is the strongest structure supporting the foot arch (Ker *et al.*, 1987; Huang *et al.*, 1993).

Similarly, the effect of transecting the plantar aponeurosis showed a significant peak joint pressure change for the first cuneometatarsal and middle cuneonavicular joints in this study. This suggests that the plantar aponeurosis dominates not only the shape of the foot but also its characteristics. It is therefore possible that acquired flat foot could lead to an extensively longer plantar aponeurosis, which could, in turn, result in an increase in joint pressures of the midfoot.

It is well known that people with diabetes have a higher plantar pressure than normal people (Cavanagh *et al.*, 1991). Experimental studies verified that the diabetic bones had decreased strength and increased stiffness (Viguet-Carrin *et al.*, 2006). In addition, another *in vivo* study verified that diabetic patients show different gait patterns when compared to a control group (Mueller *et al.*, 1994). These mechanical issues could lead to the development of intrinsic risk factors of diabetic foot complications. In respect to the significantly higher peak joint pressures seen in diabetic specimens, we speculate that people with diabetes possibly have higher mechanical stresses on their foot joints when compared to healthy people. Also, the application of repetitive high joint pressures may cause further joint deformities and arch collapse in diabetic patients, which could result in the progression of complications.

For this study, we tested 22 cadaver foot specimens; however, we only acquired meaningful data from 16 specimens, because we had 6 specimen failures during the induced arch collapse walking simulation. Most specimen failures were caused by broken midfoot joints at the cuneiform bones, specifically the joints between the metatarsals and cuneiforms and between the cuneiforms and navicular. We assume that there are three possible reasons for these specimen failures. First, we had to remove some ligaments and

joint capsules around each joints in order to insert and attach pressure sensors. Removing these soft tissues could have made the foot structure weaker than those in intact conditions. In addition, we assume that this constraint could have affected the joint pressure values. Second, the cuneiform and navicular bones are located at the apex of the foot arch, where the highest compressive loading occurs during walking simulations. In particular, the second cuneiform bone is recognized as the "key stone" in maintaining bony structure at the midfoot area (Makwana, 2005). These specimen failures could be an evidence of vicious cycle synergizing arch collapse and increased joint pressure. Lastly, the physiological conditions of specimens could be one of the factors of failures. We obtained the cadaver foot specimens from older generations - less physical activities and more bone degradations in that age could have played a role in weakening the foot structure.

There were some other factors that could have influenced this study. Limitations in the control of muscles could result in differences between *in vivo* and experimental conditions. The muscles around the ankle joint have agonist and antagonist relationships in respect to each other to control the motion of foot. The limitations in the experimental muscle control could have limited the recreation of natural walking patterns and could have influenced joint pressure values. In addition, absence of intrinsic muscle control is an inherent limitation in this study. Adding more muscle controls could be a possible solution to minimize this limitation; however, there are relatively low tensions in other ankle muscles during walking. Second, only one walking model was used to recreate the walking motion in two pathologically different groups in this study, but it has been demonstrated that people with diabetes can have slightly different walking patterns

(Mueller *et al.*, 1994).

In conclusion, arch collapse results in a significant increase in joint pressures of the midfoot. In terms of the higher peak joint pressures seen in diabetic specimens, the increased mechanical impact on foot joint could be a possible risk factor in developing foot joint problems, such as Charcot joint disease.

4.7 References

Ker, R.F., Bennett, M.B., Bibby, S.R., Kester, R.C., Alexander, R.McN., 1987. The spring in the arch of the human foot. Nature 325 (7000), 147-149.

Huang, C.K., Kitaoka, H.B., An, K.N., Chao, E.Y., 1993. Biomechanical evaluation of longitudinal arch stability. Foot & Ankle 14 (6), 353-357.

Bolgla, L.A., Malone, T.R., 2004. Plantar fasciitis and the windlass mechanism: A biomechanical link to clinical practice. Journal of Athletic Training 39 (1), 77-82.

Cashmere, T., Smith, R., Hunt, A., 1999. Medial longitudinal arch of the foot: Stationary versus walking measures. Foot& Ankle International 20 (2),112-118.

Macintyre, J., Joy, E., 2000. Foot and ankle injuries in dance. Clinics in Sports Medicine 19 (2), 351-368.

Rudzki, S.J., 1997. Injuries in Australian Army recruits. Part III: The accuracy of a pretraining orthopedic screen in predicting ultimate injury outcome. Military Medicine 162 (7), 181-483.

Cowan, D.N., Jones, B.H., Robinson, J.R, 1993. Foot morphologic characteristics and risk of exercise-related injuries. Archives of Family Medicine 2 (7), 773-777.

Nachbauer, W., Nigg, B.M., 1992. Effects of arch height of the foot on ground reaction

forces in running. Medicine and Science in Sports and Exercise 24 (11), 1264-1269.

Bertani, A., Cappello, A., Benedetti, M.G., Simoncini, L., Catani, F., 1999. Flat foot functional evaluation using pattern recognition of ground reaction data. Clinical Biomechanics 14 (7), 484-493.

Kitaoka, H.B., Ahn, T.K., Luo, Z.P., An, K.N., 1997. Stability of the arch of the foot. Foot & Ankle International 18 (10), 644-648.

Kitaoka, H.B., Luo, Z.P., An, K.N., 1997. Effect of plantar fasciotomy on stability of arch of foot. Clinical orthopaedics and related research 344, 307-312.

Arangio, G.A., Chen, C., Kim, W., 1997. Effect of cutting the plantar fascia on mechanical properties of the foot. Clinical orthopaedics and related research 339, 227-231.

van Schie, C.H., Carrington, A.L., Vermigli, C., Boulton, A., 2004. Muscle weakness and foot deformities in diabetes. Diabetes Care 27 (7), 1668-1673.

Viswanathan, V., Snehalatha, C., Sivagami, M., Seena, R., Ramachandran, A., 2003. Association of limited joint mobility and high plantar pressure in diabetic foot ulceration in Asian Indians. Diabetes Research and Clinical Practice 60 (1), 57-61.

Caputo, G.M., Ulbrecht, J., Cavanagh, P.R., 1998. The charcot foot in diabetes: six key points. American Family Physician 57 (11), 2705-2710.

Guyton, G.P., Saltzman, C.L., 2001. The diabetic foot. Journal of Bone and Joint Surgery 83 (7), 1084-1096.

Wolfe, L., Stess, R.M., Graf, P.M., 1991. Dynamic pressure analysis of the diabetic charcot foot. Journal of the American Podiatric Medical Association 81 (6), 281-287.

Lee, L., Blume, P.A., Sumpio, B., 2003. Charcot joint disease in diabetes mellitus.

Annals of Vascular Surgery 17 (5), 571-580.

Giladi, M., Milgrom, C., Stein, M., 1985. The low arch, a protective factor in stress fractures. Orthopaedic Review 14, 81-84.

Jones, B.H., Knapik, J.J., 1999. Physical training and exercise-related injuries. Sports Medicine 27 (2), 111-125.

Cavanagh, P.R., Sims, D.S. Jr., Sanders, L.J., 1991. Body mass is a poor predictor of peak plantar pressure in diabetic men. Diabetes Care 14 (8), 750-755.

Viguet-Carrin, S., Garnero, P., Delmas, P.D., 2006. The role of collagen in bone strength. Osteoporosis International 17 (3), 319-336.

Mueller, M.J., Minor, S.D., Sahrmann, S.A., Schaaf, J.A., Strube, M.J., 1994. Differences in the gait characteristics of patients with diabetes and peripheral neuropathy compared with age-matched controls. Physical Therapy 74 (4), 299-313.

4.8 Acknowledgement

Funding was provided through a NASA grant (NNJ05HF55G) and NIAMS Core Center Grant (#1P30AR-050953). Brandy Wozniak, Lawrence D. Noble, Robb W. Colbrunn and Drs. Antonie J. van den Bogert and Peter R. Cavanagh provided valuable assistance.

CHAPTER V

THE IMPACT OF TIBIALIS POSTERIOR DYSFUNCTION ON JOINT PRESSURES OF THE MIDFOOT

Dong Gil Lee and Brian L. Davis

Journal of Orthopedic Research, submitted.

5.1 Preface

The intrinsic and extrinsic muscles secure bones and joints to provide leverage in the foot. Anatomically, an activation of the tibialis posterior during walking results in the rise of the medial longitudinal arch, plantar flexion of the foot, and stabilization of the tarsal joints. Due to this anatomy, the dysfunction of the tibialis posterior is recognized as the most common cause of acquired flat foot deformity, which results in gradual medial longitudinal arch collapse, serious medial foot pain and osteoarthritis. However, the magnitudes of pressure changes in the medial foot joints during this progressive flat foot deformity process have never been quantified. In this study, we evaluated joint pressure changes for two groups (control and diabetic), where the tibialis posterior dysfunction during gait can be simulated with a robotic system.

5.2 Abstract

Tibialis posterior dysfunction is the most common cause of acquired flat foot deformity, and results in significant medial foot pain and osteoarthritis. In diabetic patients, muscle weakness is thought to be one of the contributing factors in the etiology of Charcot foot deformities. Physiologically, the loss of tibialis posterior results in a gradual collapse of the medial longitudinal arch. However, the degree of mechanical pressure change in the medial joints of the midfoot during this progressive flat foot deformity process is not completely understood. In this study, it was hypothesized that the acquired flat foot would have increased medial joint pressure. In addition, we hypothesized that diabetic specimens would have higher peak joint pressures of the midfoot than a control group. Sixteen cadaver foot specimens (8 normal/ 8 diabetic) were evaluated based on the peak joint pressure changes, where the tibialis posterior dysfunction can be introduced during simulated gait with a robotic system. Full stance walking was simulated at ¼ of the speed (averaged stance duration of 3.2s) with 66.7% body weight. Four medial joints of the midfoot (the first cuneometatarsal, medial cuneonavicular, middle cuneonavicular, and first intercuneiform) were chosen to assess the peak pressure. Evaluation of the effect of the tibialis posterior dysfunction on the peak joint pressure showed that the first cuneometatarsal, medial cuneonavicular, and middle cuneonavicular exhibited statistically significant results ($p=0.0045$, $p=0.0010$, and $p=0.0283$ respectively). In addition, all four tested joints demonstrated the elevation of peak pressures in the tibialis posterior dysfunction by 9%, 24%, 6%, and 8% respectively. Assessment of the effect of diabetes on the peak joint pressure demonstrated that diabetes have a significant impact on the both medial cuneonavicular and middle

cuneonavicular joints (p=0.0401 and p=0.0045 respectively). Across all of the tested joints, the diabetic specimen group had 51% higher peak joint pressure compared to the control specimen group over all conditions. These results suggest that increased peak joint pressures of the midfoot during simulated tibialis posterior dysfunction could be associated with flat foot syndrome. In addition, it is suggested that diabetes is an independent factor compounding the effects of tibialis posterior dysfunction.

5.3 Introduction

Acquired flat foot deformity in adults is a progressive condition resulting in pain, loss of function, and gait abnormality. The dysfunction of tibialis posterior is the most common cause of the acquired flat foot deformity. There are various risk factors associated with this condition: tendon inflammation, tendon degeneration, lack of vascularity on tendon, repeated micro-trauma on tendon, and diabetes mellitus (Hintermann, 1997). However, nearly all cases are not associated with a specific etiology (Popovic *et al.*, 2003). Interestingly, it has been suggested that the tibialis posterior dysfunction might be a common foot condition in women in the range of seventy to eighty years old (Kohls-Gatzoulis *et al.*, 2004). Generally, the progress of tibialis posterior dysfunction is classified by four steps based on the formulated treatment plan (Kohls-Gatzoulis *et al.*, 2004). Stage I is characterized by medial foot pain and swelling without any radiological deformities. Stage II is associated with the degeneration and lengthening of tendon, which occurs with the flexible deformity and medial foot pain. Stages III and IV, which vary in their degree of severity, are the end stages involving fixed deformity, significant medial foot pain and osteoarthritis. This classification

provides a better understanding about the progressive flat foot deformity; however, the relationship between mechanical pressure change in the medial foot joints and tibialis posterior dysfunction is not completely understood.

The intrinsic and extrinsic muscles secure bones and joints to provide leverage in the foot (Fiolkowski *et al.*, 2003). Anatomically, the tibialis posterior originates from the posterior region of the fibula, runs to the medial side of ankle joint, passes around the medial boundary of the tarsal joints, and inserts on the plantar aspect of the navicular and cuneiform bones. Due to this anatomy, activation of the tibialis posterior during walking results in the rise of the medial longitudinal arch, inversion and plantar flexion of the foot, and stabilization of the tarsal joints (Popovic *et al.*, 2003). The loss of this dynamic stabilizer function for the medial longitudinal arch requires additional muscle to compensate for the loss in leverage. For example, it has been suggested that a pronated foot requires greater muscle activity to stabilize the transverse tarsal joints than does the normal foot (Mann *et al.*, 1964). As a result, people with the tibialis posterior dysfunction experience more fatigue during walking. For these reasons, we hypothesized that the acquired flat foot might have an increased medial joint pressure. In addition, it was hypothesized that diabetic specimens would have higher joint pressure than normal specimens. The purpose of this study was to evaluate the joint pressures changes for two groups (normal/diabetic), where tibialis posterior dysfunction can be introduced during a simulated gait using cadaver specimens and a robotic system.

5.4 Research methods and design

Generation of Walking Model, Experimental Set-up, and Specimen Information

Generation of walking model, experimental set-up, and specimen information were described in Chapter 3.4.

Measurement Protocol

Four medial joints of the midfoot (the first cuneometatarsal, medial cuneonavicular, middle cuneonavicular, and first intercuneiform) were chosen for this study due to the functional importance of the first ray and structural importance of the second cuneiform (Cornwall *et al.*, 2004; Makwana, 2005). Pressure sensors were carefully inserted into each joint and attached on the adjacent bone surface directly using super glue.

Full stance of human gait at ¼ speeds (averaged stance duration of 3.2s) with 66.7% body weight was simulated by the UMS. In order to assess the effect of tibialis posterior dysfunction on the joint pressure of the midfoot, after collecting baseline data on the fully actuated foot, the UMS ran the same gait profiles without the tibialis posterior by deactivating the tibialis posterior tendon actuator.

Statistical Analysis

The data was analyzed using the methods of repeat measures mixed models. The variables to be used in the analysis were checked for independence using the regression diagnosis of variance inflation and condition indices. All pairwise comparisons of least square means were made using the Tukey-Kramer adjustment for multiple comparisons. The software used was SAS version 9.2 (SAS Institute Inc, Cary, North Carolina).

5.5 Results

For each group, the peak joint pressures at the middle cuneonavicular showed the highest values. The first cuneometatarsal, medial cuneonavicular, and middle cuneonavicular exhibited statistically significant peak joint pressure changes in the tibialis posterior dysfunction conditions ($p=0.0045$, $p=0.0010$, and $p=0.0283$ respectively) (from Figure 5.1 to Figure 5.3). The first intercuneiform showed the lowest peak joint pressures during the walking simulation and no statistical significant peak pressure change in the tibialis posterior dysfunction condition ($p=0.1965$) (Figure 5.4). All tested joints demonstrated peak pressure increases in the tibialis posterior dysfunction condition (9%, 24%, 6%, and 8% respectively).

Over all, the diabetic specimen group had higher peak joint pressures than the control group. The medial cuneonavicular and middle cuneonavicular exhibited significant effects of diabetes on the peak joint pressure ($p=0.0401$ and $p=0.0045$ respectively). Across all of the tested joints, the diabetic specimen group had 51% higher peak joint pressure compared to the control specimen group.

Analysis demonstrated that only the medial cuneonavicular joint was affected by the combined effect. Statistical results were provided from Table 5.1 to Table 5.4 [Diabetes in the tables (0: non-diabetic) and (1: diabetic), Specimen Condition in the tables (0: intact) and (1: tibialis posterior dysfunction)].

Table 5.1. Analysis for the first cuneometatarsal joint.

Effect	P-Value
Diabetes	0.3345
Specimen Condition	**0.0045**
Diabetes*Spec_Con	0.5462

Effect	Diabetes	Specimen Condition	LS Mean
Diabetes	0	-	3.8548
Diabetes	1	-	5.7598
Specimen Condition	-	0	4.6056
Specimen Condition	-	1	5.0090
Diabetes*Spec_Con	0	0	3.6827
Diabetes*Spec_Con	0	1	4.0269
Diabetes*Spec_Con	1	0	5.5285
Diabetes*Spec_Con	1	1	5.9911

Table 5.2. Analysis for the medial cuneonavicular joint.

Effect	P-Value
Diabetes	**0.0401**
Specimen Condition	**0.0010**
Diabetes*Spec_Con	**0.0467**

Effect	Diabetes	Specimen Condition	LS Mean
Diabetes	0	-	2.8095
Diabetes	1	-	5.7286
Specimen Condition	-	0	3.8190
Specimen Condition	-	1	4.7191
Diabetes*Spec_Con	0	0	2.5760
Diabetes*Spec_Con	0	1	3.0431
Diabetes*Spec_Con	1	0	5.0620
Diabetes*Spec_Con	1	1	6.3951

Effect	Diabetes	Spec_Con	Diabetes	Spec_Con	P-Value
Diabetes*Spec_Con	0	0	0	1	0.5416
Diabetes*Spec_Con	0	0	1	0	0.2355
Diabetes*Spec_Con	0	0	1	1	**0.0273**
Diabetes*Spec_Con	0	1	1	0	0.4109
Diabetes*Spec_Con	0	1	1	1	0.0587
Diabetes*Spec_Con	1	0	1	1	**0.0008**

Table 5.3. Analysis for the middle cuneonavicular joint.

Effect	P-Value		
Diabetes	**0.0045**		
Specimen Condition	**0.0283**		
Diabetes*Spec_Con	0.5756		
Effect	**Diabetes**	**Specimen Condition**	**LS Mean**
Diabetes	0	-	4.7824
Diabetes	1	-	8.3873
Specimen Condition	-	0	6.3783
Specimen Condition	-	1	6.7914
Diabetes*Spec_Con	0	0	4.5346
Diabetes*Spec_Con	0	1	5.0301
Diabetes*Spec_Con	1	0	8.2219
Diabetes*Spec_Con	1	1	8.5527

Table 5.4. Analysis for the first intercuneiform joint.

Effect	P-Value		
Diabetes	0.5857		
Specimen Condition	0.1965		
Diabetes*Spec_Con	0.1602		
Effect	**Diabetes**	**Specimen Condition**	**LS Mean**
Diabetes	0	-	1.5232
Diabetes	1	-	1.1467
Specimen Condition	-	0	1.2845
Specimen Condition	-	1	1.3854
Diabetes*Spec_Con	0	0	1.4320
Diabetes*Spec_Con	0	1	1.6144
Diabetes*Spec_Con	1	0	1.1370
Diabetes*Spec_Con	1	1	1.1564

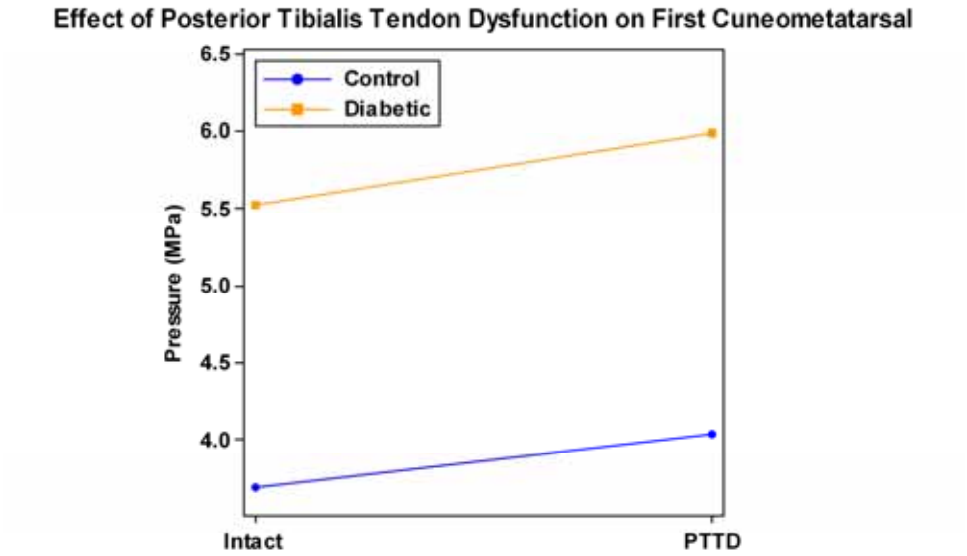

Figure 5.1. Effect of posterior tibialis tendon dysfunction on the first cuneometatarsal joint.

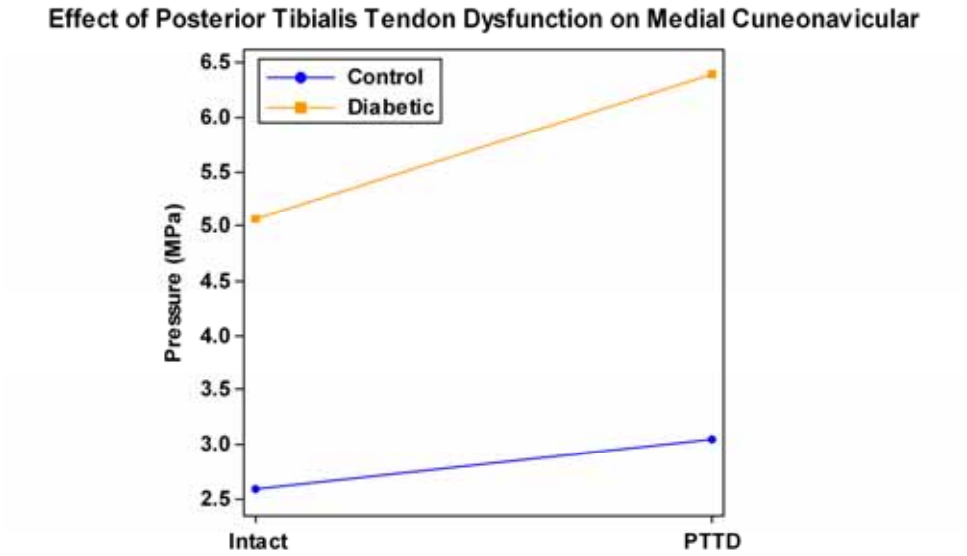

Figure 5.2. Effect of posterior tibialis tendon dysfunction on the medial cuneonavicular joint.

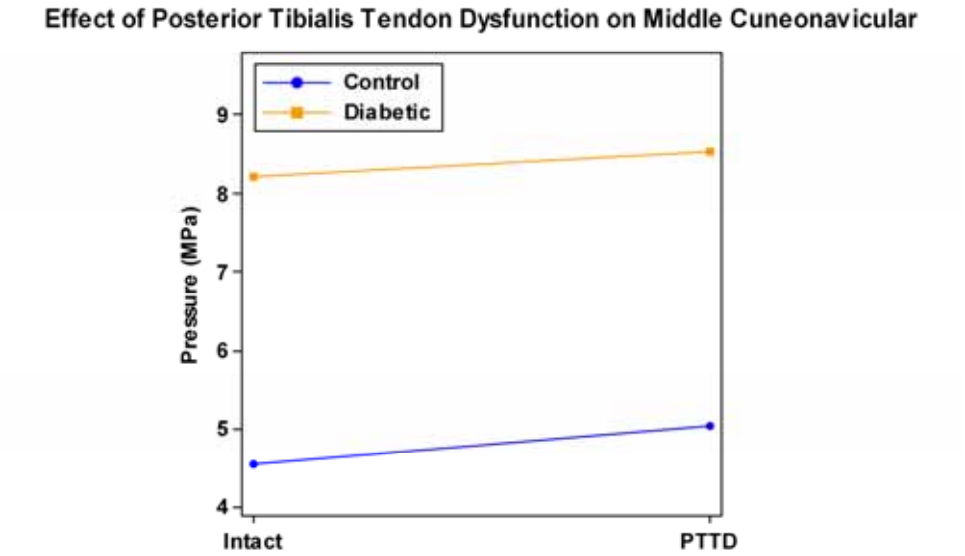

Figure 5.3. Effect of posterior tibialis tendon dysfunction on the middle cuneonavicular joint.

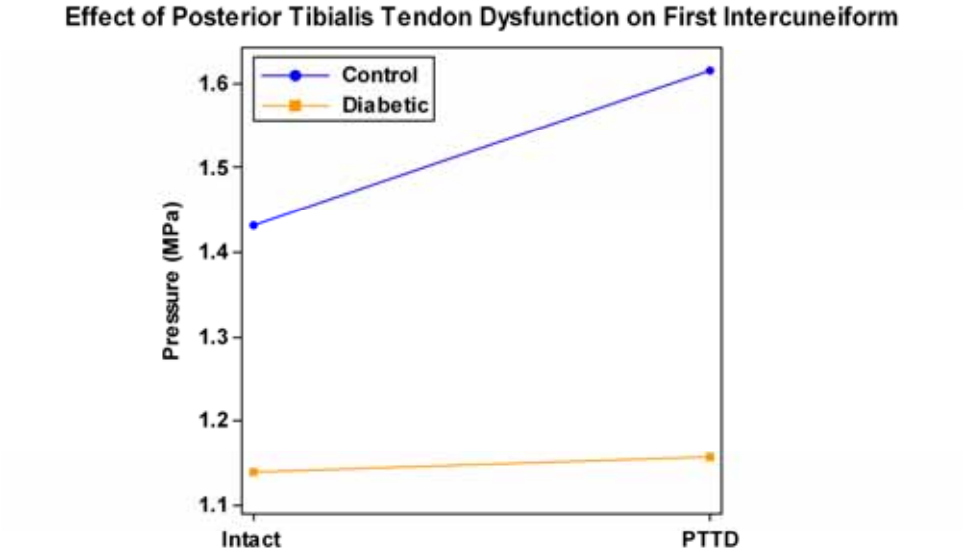

Figure 5.4. Effect of posterior tibialis tendon dysfunction on the first intercuneiform joint.

5.6 Discussion

The robotic gait simulation with cadaver specimen provides a unique opportunity to investigate both internal and external foot biomechanics. A well established experimental protocol offers repeatability and minimizes clinical variations (Sharkey *et al.*, 1998). The use of cadaver specimen provides characteristics similar to the natural tissue structures and properties as well. One of the most attractive aspects of the robotic gait simulation is the fidelity in re-creating physiological/biomechanical conditions that mimic actual gait. This allows physicians to verity the effectiveness of surgical treatments before the actual surgery. For example, a tendon transfer is one of the surgical interventions in the case of tibialis posterior dysfunction. The robotic system could be used to find out an optimized method of the tendon transfer by simulating walking after the surgical trial on a cadaver specimen.

In the current study, the robotic gait simulator was used to investigate the interaction between bones, muscles and joint pressures. As expected, the peak joint pressures of the midfoot increased considerably in the tibialis posterior dysfunction compared to the intact condition. This result suggests that the increased peak joint pressures could be associated with midfoot pain in the acquired flat foot syndrome. In particular, the location of the most significant peak joint pressure increase, the medial cuneonavicular, could be related to the anatomical location of the tibialis posterior. The activation of tibialis posterior during gait results in the increase of medial longitudinal arch by supporting the navicular and cuneiform bones. Since the insertion of tibialis posterior is on the plantar aspect of the navicular and cuneiform bones, the dysfunction of tibialis posterior could result in large kinematic and kinetic changes of medial

navicular and cuneiform bones during gait. This is in accordance with Thordarson *et al.*, (1995) who verified the effect of tibialis posterior on kinematic changes of midfoot joints at a certain phase of gait (static condition). While they used a static loading scenario, we have demonstrated the effect of tibialis posterior on joint pressures of the midfoot at the full phase of gait (dynamic condition).

Foot problems are common debilitating conditions in diabetic patients suffering from neuropathies. It has been investigated that diabetes generates highly cross-linked proteins that stiffens tissues (Sullivan *et al.*, 2005; Giacomozzi *et al.*, 2005). The changes in tissue structures were assumed to be a biological cause of the limited range of motion in diabetic patients (D'Ambrogi *et al.*, 2003). In addition, it has been verified that the limited range of motion in diabetes results in a higher plantar pressure during walking (Cavanagh *et al.*, 1991). These biological and mechanical issues were assumed to be the leading causes of diabetic foot problems. We speculated that significantly higher peak joint pressures of the midfoot in diabetic specimens in this study could be associated with these biological and mechanical issues.

In this study, we simulated two different physiological foot conditions using the UMS. The dysfunction of tibialis posterior was simulated by deactivating the tibialis posterior tendon actuator. Nonetheless, this experimental method has some fundamental limitations to simulate the tibialis posterior dysfunction. First, it has not been fully verified whether the tibialis posterior dysfunction stands for "no function" or "abnormal function" in the biomechanical point of view. A rupture of the tibialis posterior could be categorized as "no function"; however, an elongation of the tibialis posterior might be classified as "abnormal function". For this reason, it is necessary to investigate both the

activation and function of tibialis posterior from the acquired flat foot population for further studies. Second, it has not been verified that the loss of tibialis posterior affects activities in other muscles. It has been suggested that the pronated foot requires a greater muscle activity (Mann *et al.*, 1964). This finding could have a thread of connection, which links to the development of lower extremity fatigue in people with flat foot. In addition, it is also possible there are alternative actions of other muscles to compensate for the tibialis posterior dysfunction; however, such muscular compensations have not been investigated in people with the tibialis posterior dysfunction. Furthermore, people with tibialis posterior dysfunction could have different walking patterns than that of the normal population; however, we used only one walking pattern to simulate both normal and the tibialis posterior dysfunction. Lastly, the dysfunction of tibialis posterior could lead to series of characteristic changes in soft tissues. For example, ligaments might function differently under the increased tension during a gradual arch collapsing. Repetitions of this increased tension could result in the lengthening of ligaments and formation of different arrangements of bones. Transecting the parts of ligaments in cadaver specimens could be a possible solution to mimic this anatomical foot condition.

Despite the limitations of using the UMS, this study is the first to examine the combined effects of diabetes and posterior tibial dysfunction on joint pressures of the midfoot. Our results strongly suggest that these are compounding factors that place joints of the midfoot at increased risk for bony collapse due to elevated stresses.

5.7 References

Hintermann, B., 1997. Tibialis posterior dysfunction: a review of the problem and personal experience. Foot and Ankle Surgery 3 (2), 61-70.

Popovic, N., Lemaire, R., 2003. Acquired flatfoot deformity secondary to dysfunction of the tibialis posterior tendon. Acta Orthopaedica Belgica 69 (3), 211-221.

Kohls-Gatzoulis, J., Angel, J., Singh, D., 2004. Tibialis posterior dysfunction as a cause of flatfoot in elderly patients. The Foot 14 (4), 207-209.

Kohls-Gatzoulis, J., Angel, J., Singh, D., Haddad, F., Livingstone, J., Berry, G., 2004. Tibialis posterior dysfunction: a common and treatable cause of adult acquired flatfoot. British Medical Journal 329 (7478), 1328-1333.

Fiolkowski, P., Brunt, D., Bishop, M., Woo, R., Horodyski, M., 2003. Intrinsic pedal musculature support of the medial longitudinal arch: an electromyography study. Journal of Foot and Ankle Surgery 42 (6), 327-333.

Mann, R., Inman, V. T., 1964. Phasic activity of intrinsic muscles of the foot. The Journal of bone and joint surgery 46 (3), 469-481.

Sharkey, N.A., Hamel, A.J., 1998. A dynamic cadaver model of the stance phase of gait: performance characteristics and kinetic validation. Clinical Biomechanics 13 (6), 420-433.

Thordarson, D.B., Schmotzer, H., Chon, J., Peters, J., 1995. Dynamic support of the human longitudinal arch. Clinical orthopaedics and related research 316, 165-172.

Sullivan, K.A., Feldman, E.L., 2005. New developments in diabetic neuropathy. Current Opinion in Neurology 18 (5), 586-590.

Giacomozzi, C., D'Ambrogi, E., Uccioli, L., Macellari, V., 2005. Does the thickening of

Achilles tendon and plantar fascia contribute to the alteration of diabetic foot loading? Clinical Biomechanics 20 (5), 532-539.

D'Ambrogi, E., Macellari, V.M., Giurato, L., Caselli, A., D'Agostino, M.A., Ucciolo, L., Giacomozzi, C., 2003. Contribution of plantar fascia to the increased forefoot pressures in diabetic patients. Diabetes Care 26 (5), 1525-1529

Cavanagh, P.R., Sims, D.S. Jr., Sanders, L.J., 1991. Body mass is a poor predictor of peak plantar pressure in diabetic men. Diabetes Care 14 (8), 750-755.

5.8 Acknowledgment

Funding was provided through a NASA grant (NNJ05HF55G) and NIAMS Core Center Grant (#1P30AR-050953). Brandy Wozniak, Lawrence D. Noble, Robb W. Colbrunn and Drs. Antonie J. van den Bogert and Peter R. Cavanagh provided valuable assistance.

CHAPTER VI

CONCLUSIONS

6.1 Summary

The most common situation in which diabetic foot problems develop involves a combination of intrinsic physiological factors and extrinsic mechanical factors. For example, a diabetic patient who has reduced sensation in his/her foot has a higher chance of developing foot problems. This occurs because the patient continues to walk with higher plantar pressures that are caused by abnormal loading, due to diabetic joint and tissue complications. In addition, poor blood circulation of the diabetic foot prevents the healing process. Therefore, the common reasons for diabetic foot complications can be summarized as neuropathy, repeated higher mechanical loading, and poor healing. In this study, we focused on medial joint pressures which are considered as one of the mechanical risk factors.

It was verified that the diabetic specimen group had significantly higher joint pressures of the midfoot than the non-diabetic control group for both (i) intact and (ii) simulated arch-collapse conditions. This finding implies that people with diabetes could

have higher mechanical stresses on their joints of the midfoot than non-diabetic people during daily activities. In addition, application of the repetitive high joint pressures in diabetic feet could result in initiation and acceleration of joint problems. This result suggests that patients with diabetes are predisposed to mechanical alterations in the arch of their feet, even without visible signs of midfoot collapse.

We found an inverse correlation between arch height and joint pressures of the midfoot in Chapter IV. This study was based on the idea that an arch collapse could be simulated by an altered ligamentous arch support. This result supported our hypothesis; that the mechanics of the altered foot could result in an increased joint stress during gait. In particular, the gradual joint pressure increase of the midfoot during arch collapse in diabetic patients could result in the progression of serious complications. One such complication being an Charcot foot abnormality. The results of this study could be used to further our understanding of the etiology of diabetic foot disease and suggest better treatment options for diabetic patients, who are at a higher risk for developing foot problems.

It was proven that the acquired flat foot, caused by the tibialis posterior dysfunction, caused medial joint pressure increase. We assumed that the location of the major insertion of the tibialis posterior, on the plantar aspect of the navicular and cuneiform bones, could result in large kinematic and kinetic changes of the medial bones of the midfoot during gait. This result suggests that increased peak joint pressures of the midfoot, with the tibialis posterior dysfunction, could be associated with midfoot pain in the acquired flat foot syndrome.

6.2 Novel contributions

From a clinical standpoint, this study disclosed a significant risk factor, namely higher joint pressure of the midfoot, in diabetic foot complications. In addition, this study revealed the relationship between arch height and joint pressures of the midfoot during induced arch collapse during dynamic walking trials. From an engineering point of view, this study demonstrated a potent possibility of using the robotic system in biomechanical applications. Theses findings and accomplishments can be stated as;

1. The control software was successfully developed to control the universal musculoskeletal simulator (UMS) for the various human walking simulation studies.
2. Diabetic cadaver feet had, on average, 46% higher medial peak joint pressures of the midfoot than control cadaver feet during simulated stance.
3. There were inverse correlations between the arch height and the peak medial joint pressures during the simulated arch collapse experiment.
4. Medial joints of the midfoot demonstrated a 12% elevation of peak pressure in the tibialis posterior dysfunction experiment.

These findings suggest that the application of repetitive high joint pressures may cause joint deformities and arch collapse in diabetic patients, which could eventually result in the progression of problems, such as Charcot foot abnormalities. In addition, ligaments and muscles not only act as a bow-string to maintain the shape of the foot arch, but also contribute a significant effect on determining foot joint stability.

6.3 Assumptions and limitations

Cadaver simulation studies have some common inherent limitations (i) different tissue textures from the living tissue (ii) limited information about a donor's activity and history (iii) some unnatural kinematics compared with a living subject's motion (iv) large variations from specimen to specimen. In order to minimize these limitations, the vertical ground-reaction-force was tightly optimized and controlled to keep within a 10% error range. This contributed to good simulation trial-to-trial repeatability.

For some specimens, the physiological conditions were one of the factors leading to failure during walking simulation. We obtained the cadaver foot specimens from older generations - less physical activities and more osteoporosis in this age group could have played a role in weakening the foot structure. In terms of a walking model, only one non-diabetic living subject's walking was used for the desired walking pattern to recreate walking motion for both non-diabetic and diabetic specimen groups.

Lack of intrinsic muscle control was an innate limitation of this study because only five extrinsic muscles were used to provide muscle forces during walking simulation. However, each extrinsic muscle force was optimized and adjusted independently to compensate for the limited number of muscles. The pressure sensor insertion procedure required sacrifice of surrounding soft tissue during the incision which could have affected the stability of the foot structure. We transected and deactivated ligaments and tendons to simulate arch collapsing that was not comparable to a realistic and natural arch collapsing conditions. Lastly, we simulated walking with 25% walking speed and 66.7% body weight, because of the hardware limitation of the UMS and the dynamic range limitation of the pressure sensors.

6.4 Future work

In order to overcome limitation of the cadaver specimen, it is necessary to investigate a donor's physiological histories such as level of physical activities and existence of bone diseases. Cadaver specimens of younger generations could provide a stronger and more reliable reference; whereas, older generation specimens are more likely to incur bone damage during experimentation. Therefore, it is necessary to get the cadaver foot specimens from younger generations for future studies. In addition, we found large specimen to specimen variations in joint pressure values. In order to overcome this limitation, it might be helpful to obtain more cadaver specimens for future studies.

Since this study only used one walking model for different specimen groups, *in vivo* studies are required to make appropriate walking models for different groups to more accurately simulate walking patterns. For example, it would be preferable for the robotic system to simulate an averaged diabetic walking pattern for diabetic specimens. In addition, it is required to investigate anatomical and functional activity of ligaments and tendons from the acquired flat foot population for a better simulation of arch collapse.

This study demonstrated a potent ability of using the robotic system to verify surgical interventions in clinical applications. First of all, this study successfully verified effects of the plantar fasciotomy on joint pressures of the midfoot. The elongation of the plantar aponeurosis could not only develop higher pressure values on the midfoot but also result in various mechanical effects on the foot such as lengthening of soft tissues on the plantar aspect. This ultimately results in a longer lever arm during walking. These changes could be related to the medial foot pain after the plantar fasciotomy. Second, this

robotic system could be used to determine the effect of tendon transfer surgery which is an option for people with tibialis posterior dysfunction. In addition, this robotic system could be used to verify the effect of tendon lengthening and shortening interventions on key biomechanical parameters pertaining to foot function.

This robotic system has the ability to simulate various lower extremity motions such as walking, landing, and cycling. It is known that women have larger Q-angle and more chance to develop knee injuries. Many researchers have focused on the relationship between bone orientation and knee injury mechanism. This robotic system could be used to study injury mechanisms on the knee and ankle during landing simulation. It could also be used to simulate and prove the effect of rehabilitation treatments.

Finally, realistic mechanical testing for implants, orthodics, and prosthesis would be valuable to determine performance of medical devices. This robotic system could be used as an *in vitro, in situ* testing machine by simulating various motions to measure performance of various medical devices.